nature reviews earth & environment

https://doi.org/10.1038/s43017-023-00509-7

Review article

Check for updates

Short- and long-term variability of the Antarctic and Greenland ice sheets

Edward Hanna[1] ✉, Dániel Topál[2,3], Jason E. Box[4], Sammie Buzzard[5,6], Frazer D. W. Christie[7], Christine Hvidberg[8], Mathieu Morlighem[9], Laura De Santis[10], Alessandro Silvano[11], Florence Colleoni[10], Ingo Sasgen[12,13], Alison F. Banwell[14], Michiel R. van den Broeke[15], Robert DeConto[16], Jan De Rydt[6], Heiko Goelzer[17], Alexandra Gossart[18], G. Hilmar Gudmundsson[6], Katrin Lindbäck[19,20], Bertie Miles[21], Ruth Mottram[22], Frank Pattyn[23], Ronja Reese[6], Eric Rignot[24,25,26], Aakriti Srivastava[27], Sainan Sun[6], Justin Toller[28], Peter A. Tuckett[29] & Lizz Ultee[30]

Abstract

The variability of the Antarctic and Greenland ice sheets occurs on various timescales and is important for projections of sea level rise; however, there are substantial uncertainties concerning future ice-sheet mass changes. In this Review, we explore the degree to which short-term fluctuations and extreme glaciological events reflect the ice sheets' long-term evolution and response to ongoing climate change. Short-term (decadal or shorter) variations in atmospheric or oceanic conditions can trigger amplifying feedbacks that increase the sensitivity of ice sheets to climate change. For example, variability in ocean-induced and atmosphere-induced melting can trigger ice thinning, retreat and/or collapse of ice shelves, grounding-line retreat, and ice flow acceleration. The Antarctic Ice Sheet is especially prone to increased melting and ice sheet collapse from warm ocean currents, which could be accentuated with increased climate variability. In Greenland both high and low melt anomalies have been observed since 2012, highlighting the influence of increased interannual climate variability on extreme glaciological events and ice sheet evolution. Failing to adequately account for such variability can result in biased projections of multi-decadal ice mass loss. Therefore, future research should aim to improve climate and ocean observations and models, and develop sophisticated ice sheet models that are directly constrained by observational records and can capture ice dynamical changes across various timescales.

Sections

A full list of affiliations appears at the end of the paper. ✉e-mail: ehanna@lincoln.ac.uk

Introduction

Ice sheet mass budget is a function of surface mass balance (net snow accumulation minus the runoff of surface meltwater), basal mass balance (net mass change owing to accumulation and melting at the base of an ice sheet or ice shelf), and dynamics (ice flow and calving). This mass balance has been negative for both the Antarctic Ice Sheet (AIS) and Greenland Ice Sheet (GrIS) for several decades, with individual rates estimated at -127 ± 23 Gt year^{-1} and -255 ± 19 Gt year^{-1}, respectively, from 2002 to 2022 (Fig. 1), totalling -382 ± 42 Gt year^{-1} (~1.1 mm year^{-1} sea level equivalent). As such, the ice sheets have together overtaken mountain glaciers as the dominant cryospheric contributor[1] to the global mean sea level rise of approximately 3.3 mm year^{-1} over 2002–2020 (ref. 2).

Embedded within these long-term negative mass loss trends are considerable well-documented short-term fluctuations in ice mass[3] (Fig. 1). These short-term fluctuations include the break-up and collapse of the Larsen A (1995), Larsen B (2002) and Wilkins (2008) ice shelves in the AIS[4,5] and the major surface melt events in 2010, 2012 and 2019 across the GrIS[6]. In the case of the latter, these relatively short-term melt events lasting a few days to a few weeks can produce annual mass loss anomalies double those of surrounding years, as in July 2012 and July and August 2019 (Fig. 1b). However, it remains unclear how indicative such short-term extreme events are of longer-term change and what the impact of system-intrinsic variability (that is, sub-daily to decadal timescale variations in atmosphere and ocean circulation and ice dynamics) is compared with that of longer-term external forcing (especially climate change over decades or centuries).

The different impacts of long-term and short-term variability — coupled with the fact that ice sheet model forcing often excludes extremes or variances — contribute substantial uncertainties to projections of future ice sheet mass change. Given that mass loss projections underpin sea level projections, these uncertainties have important ramifications for climate adaptation (for example, coastal protection strategies) and mitigation.

In this Review, we use observational and model evidence of ice sheet change to understand how short-term and long-term effects contribute to ice sheet change. We first outline the key atmospheric and oceanic drivers and hydrological processes that are involved in ice sheet change. Next, we explore short-term and long-term changes in the AIS and GrIS and the interrelations between these timescales that can provide insight into ice sheet sensitivity and response to ongoing climate warming. Last, we recommend research priorities.

Drivers and processes of ice sheet mass change

Ice sheet mass change is driven by several processes (Fig. 2), including variations in atmospheric and oceanic forcing, hydrology and sea ice, and by ice sheet instabilities, as now discussed.

Atmospheric forcing

The atmosphere affects the mass balance of ice sheets on a range of spatial (sub-metre to hundreds of kilometres) and temporal (sub-minute to decadal) scales (Fig. 2). Atmospheric circulation impacts ice sheets primarily through its direct influence on accumulation and ablation, regulating snow and rainfall and the surface energy balance.

Snow accumulation on the AIS and GrIS exhibits a strong gradient. Accumulation is largest at the ice sheet margin, locally reaching >1 m year^{-1} water equivalent; in-air sublimation in the dry polar atmosphere[7] and sublimation and erosion by near-surface (katabatic and foehn) winds[8,9] can introduce substantial small-scale spatial variability. Generally, high accumulation is linked to synoptic scale systems, including atmospheric rivers (episodic narrow bands of enhanced moisture transport) that are associated with large amounts of snowfall[10–12]. Indeed, the top 10% of daily precipitation totals for the AIS contribute around half of the total annual precipitation, dominating surface mass balance, especially in coastal areas and over the ice shelves[13]. Precipitation across the south-eastern GrIS and Antarctic Peninsula is also linked to topographic lifting of relatively warm and moist air masses[14,15]. From these high coastal accumulation rates, snowfall decreases markedly to <10 cm year^{-1} water equivalent towards the elevated interiors wherein colder and drier conditions prevail and precipitation falls primarily as diamond dust[16,17].

Accumulation and ablation are also influenced by modes of climate variability. For instance, surface melt events in the GrIS are tightly coupled to the North Atlantic Oscillation. A trend towards negative phases since the 1990s (ref. 18) has been accompanied by more anticyclonic circulation anomalies (blocking events), the descending air and adiabatic warming of which lead to extreme melt episodes[19,20], especially in conjunction with low-level warm air advection[21], shallow surface-based temperature inversions[22] and accompanying cloud-radiative anomalies[23,24]. These blocking events are also thought to be partially linked to Pacific decadal variability[25], as well as on higher-frequency timescales associated with El Niño Southern Oscillation changes. Blocking highs over Greenland deflect the atmospheric jet stream and synoptic weather systems further south over the North Atlantic, reducing accumulation over southern Greenland in summer but increasing it in western Greenland in winter[26].

Modes of climate variability are similarly important in Antarctica, dominating interannual surface mass balance variability[27]. In particular, a trend towards positive phases of the Southern Annular Mode from the 1950s to the 2010s (ref. 28) — driven by stratospheric ozone depletion and greenhouse gas emissions and modulated by multi-decadal variability in Pacific and Atlantic sea surface temperature — is associated with stronger westerly winds, enhanced circumpolar deep water upwelling[29] and, thereby, ice shelf basal melting[30]. In addition to impacting ablation, the Southern Annular Mode trend also influences accumulation, although the observed increase in Antarctic snow accumulation since 1900 could be caused by other factors[31].

The response of the ice sheet to atmospheric forcing is modulated by the firn layer — a layer of buried snow (up to 120 m thick), which slowly (decades to millennia) transforms into ice[32,33]. This firn layer acts as a low-pass filter between short-term atmospheric variability in snowfall, which replenishes the firn pore space, and melt, which destroys it. Refreezing of surface meltwater within the firn during cooler periods following warming is also critical because it caps the firn and increases runoff. Also, over the GrIS, firn layer saturation under warmer, high-melt conditions causes the expansion of the runoff zone, which can lead to accelerated mass loss. Because of the considerable year-to-year variability in melt and accumulation, this evolution of the firn layer provides a useful baseline for distinguishing ice sheet 'weather' from 'climate' changes.

Oceanic forcing

Oceanic forcing drives ice sheet mass loss by melting marine-terminating glaciers and ice shelves (Fig. 2). Both the GrIS and AIS exhibit interannual-scale to decadal-scale variability in response to oceanic forcing, potentially related to internal climate variability[34,35].

In Greenland, for example, such oceanic forcing has been implicated in the multi-decadal retreat and thinning of several coastal glaciers since at least the early 1990s, as well as decadal oscillations in their frontal position and thickness[34,36]. These glaciers largely terminate into

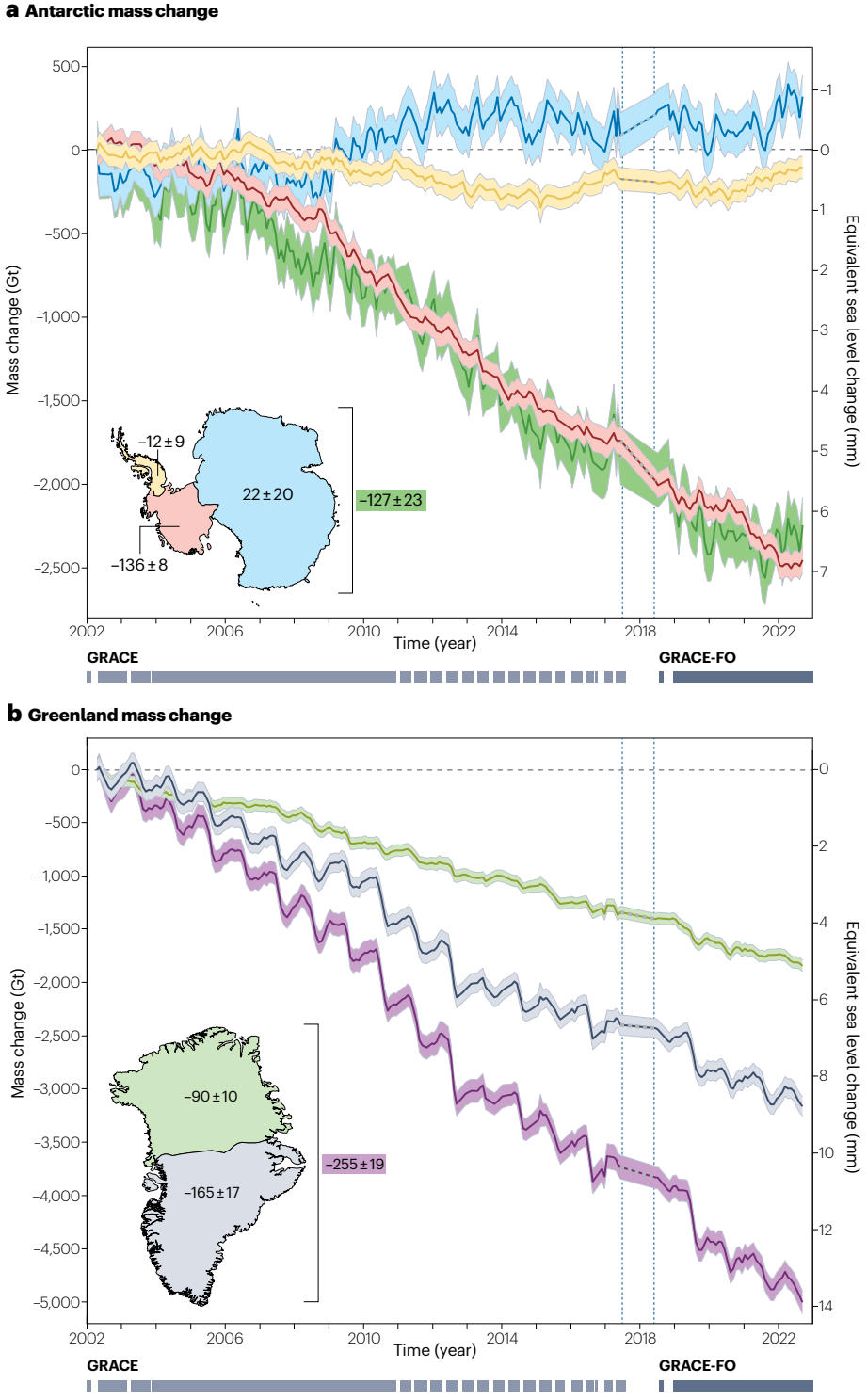

Fig. 1 | Antarctic and Greenland ice mass change. **a**, Time series of mass change and the equivalent sea level change for the Antarctic Ice Sheet for 2002–2022 based on 213 monthly gravity field solutions from GRACE/GRACE-FO[249]. Mass change estimates are provided for the entire ice sheet (green), East Antarctica (blue), West Antarctica (red) and the Antarctic Peninsula (yellow). Shading represents 2-sigma monthly empirical uncertainties. The glacial-isostatic adjustment (GIA) correction represents the arithmetic average of the models IJ05 R2 (ref. 250), AGE1 (ref. 251) and ICE-6G_D (ref. 252). The uncertainties for the mass balances on the map inset (in Gt year^{-1}) consist of propagated empirical uncertainties and the spread of 13 model corrections for GIA[249]. The vertical dashed lines indicate the end of GRACE and start of the GRACE-FO science data operations, and the coloured dashed lines within these intervals represent linear interpolations over the observational gap. **b**, The same as in part **a**, but for the Greenland Ice Sheet[184]. Estimates are provided for the entire ice sheet (purple) and the regions north (green) and south (grey) of about 72° N. The GIA correction is the GGG1.D model, tuned to fit measured GIA-induced GPS uplift rates[253]. The uncertainties on the mass balances in the map inset consist of propagated empirical uncertainties and the spread of ten model corrections for GIA[184]. The bars at the bottom indicate the measurement periods underlying the GRACE and GRACE-FO monthly gravity field solutions. Greenland lost approximately double the mass of Antarctica from 2002 to 2022, but both ice sheets exhibit substantial interannual variations in mass changes. GPS, Global Positioning System; GRACE, Gravity Recovery and Climate Experiment; GRACE-FO, GRACE-Follow-On.

fjords as cliff-like vertical ice fronts in which oceanic heat flux regulates submarine melting. Ocean heat fluxes are regulated by oceanic temperatures in the fjords and by near-glacier meltwater plumes[36]. Relatively high oceanic temperatures in the fjords are associated with inflow of Atlantic waters at depth[37]. Meanwhile, plumes develop adjacent to the ice front and originate from subglacial meltwater discharge that is ultimately driven by surface melting and subsequent runoff (which, in turn, is closely linked to atmospheric forcing[36]). Submarine melting can also indirectly cause the retreat of marine-terminating glaciers by enhancing iceberg discharge[38–40].

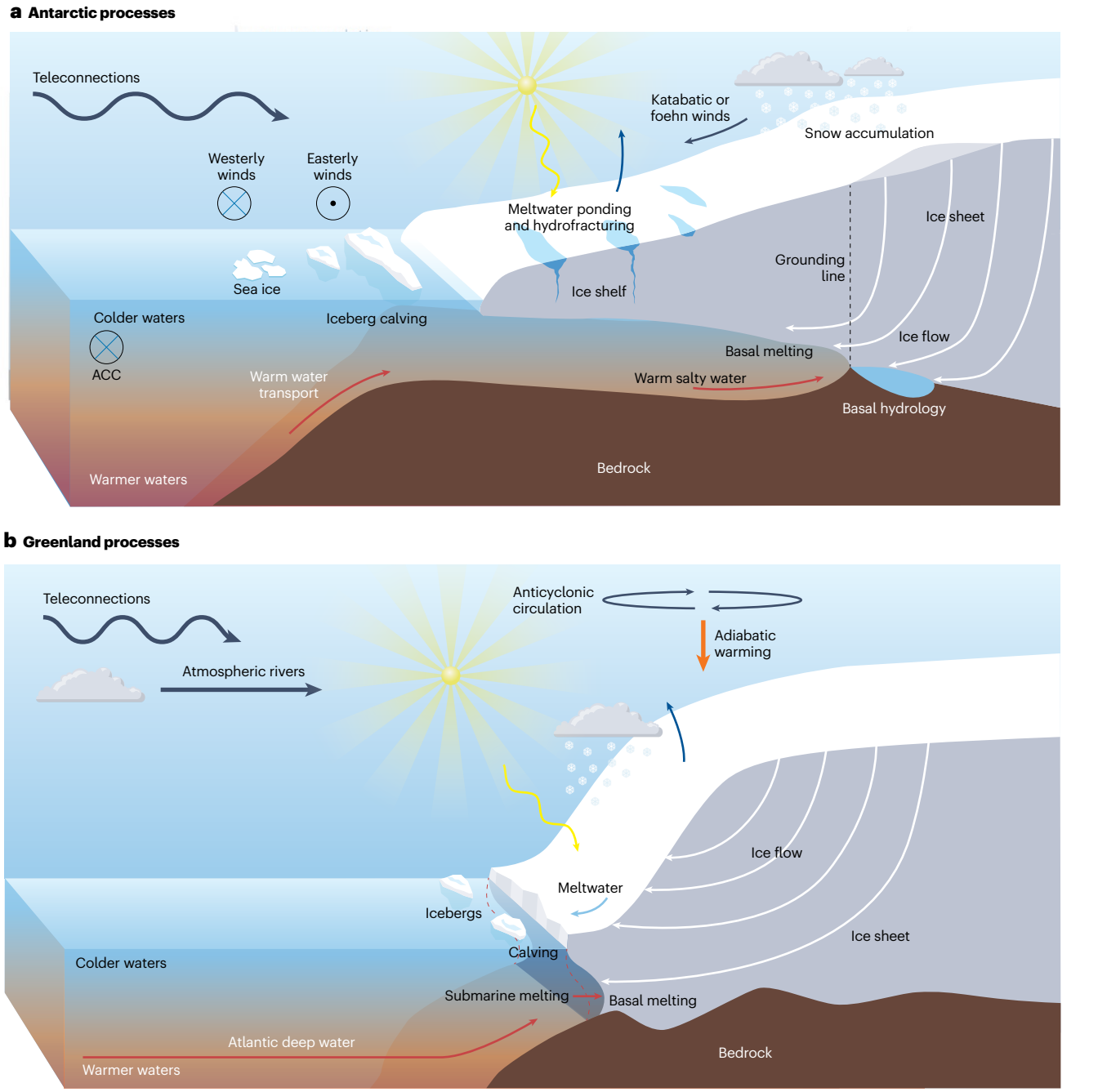

Fig. 2 | Key processes influencing ice sheet mass balance. a, Weather, climate, hydrological and ocean processes in Antarctica, including the relatively warm water flow in the ocean (red arrows), ice flow (white arrows), incoming shortwave radiation (yellow arrows) and sublimation and evaporation (dark blue arrows). **b**, The same as in part **a**, but for Greenland, with the orange arrow indicating descending atmospheric motions (adiabatic warming) in the atmosphere and the light blue arrow indicating the flow of meltwater into the ocean. Greenland is dominated by atmospheric processes, whereas oceanic forcing predominates for the Antarctic Ice Sheet. ACC, Antarctic Circumpolar Current.

By contrast, oceanic forcing of the AIS is dominated by the melting of floating ice shelves (which cover 75% of the Antarctic coast)[41]. In these cases, upwelled warmer waters are channelized towards the base of ice shelves, driving melt[29,42–44]. Indeed, much of the interannual to multi-decadal AIS mass loss has occurred in regions exhibiting ocean-driven basal melting, retreat and thinning of ice shelves[27,42–45] and outlet glaciers[46–48], particularly along coastal West Antarctica[35,44,48,49]. This process of vigorous ocean-driven melt is also implicated in the sustained retreat of the marine-terminating glaciers[49] of the Western Antarctic Peninsula. Simulations of the Amundsen Sea, West Antarctica,

over the twentieth century further confirm that oceanic forcing has become stronger[50]. In case of a sustained oceanic forcing anomaly, an ice sheet can be perturbed until its equilibrium state cannot be recovered; however, the mechanisms controlling such long-term behaviour are currently poorly understood. More generally, the role of subglacial water discharge in ice shelf basal melting remains poorly constrained, with some evidence suggesting that it can increase basal melting near the grounding zone[51,52].

Effect of sea ice on ice sheet change

Natural variability in sea ice cover can also drive changes in the ice sheet mass budget. For example, satellite observations indicate that glacial advance occurs when highly pressurized sea ice or ice mélange (a mix of sea ice and icebergs) is connected to the shelf front or tidewater glaciers, preventing calving through enhanced buttressing and reduced gravitational flow[53,54]. Sea ice cover also limits how much and how far atmospheric moisture reaches inland in the form of snowfall[55,56]. Records of such processes prior to the satellite era and their importance for longer-term ice sheet mass balance can be reconstructed from ice core proxies[57,58] and marine sediment cores[59]. These measurements are used to infer past sea ice cover and how it was influenced by changing oceanic and atmospheric frontal systems. For relatively small and thin ice shelves (including the Antarctic Peninsula's Larsen A and B ice shelves prior to their collapse), short-lived, high-energy ocean waves during times of regional, storm-driven sea ice loss can also occasionally trigger calving events[53,60].

Ice sheet hydrology

Surface melt is widespread and complex in Greenland and on Antarctica's low-lying ice shelves[61,62] (Fig. 2) and will probably become an increasingly important component of the ice sheet mass budget in a warming climate[63,64], partly owing to the melt–albedo feedback[65,66]. Although the relationship between climate and the development of surface hydrological systems over multi-annual timescales is uncertain[67], the importance of surface melt is well-established. The GrIS, for example, experiences considerable mass loss through runoff. Indeed, roughly 50% of ice lost from the GrIS from 1992 to 2018 is estimated to be from this process[42,68].

In Antarctica, surface melting is widespread only on and immediately adjacent to the ice shelves of the continent[61,69], wherein much of the melt refreezes in situ and is, therefore, not lost through runoff[42]. However, meltwater can influence ice shelf stability though the formation of surface meltwater lakes, leading to surface meltwater-driven ice shelf flexure and/or through-ice fracture (hydrofracture)[70]. Some Antarctic Peninsula ice shelves are particularly vulnerable to hydrofracture, and their future vulnerability will be partly determined by the production and destination of surface melt[71] and by snowfall, which replenishes firn pore space[72,73]. Hydrofracture-driven ice shelf disintegration events can lead to accelerated ice loss through the de-buttressing of upstream glacier ice[74].

In the GrIS and AIS, the drainage of surface melt to the bed is inferred to subsequently influence ice dynamics through connections to the subglacial hydrological system[75–77]. Generally, however, the impact of hydrodynamic coupling on ice motion for grounded ice is uncertain[75,78].

Marine ice instabilities

Marine ice sheet instability (MISI) is a self-enhancing process, which results from the interactions between grounding lines, bed topography and ice dynamics. MISI is typically triggered by the thinning of a confined ice shelf, which buttresses upstream flow, leading to grounding-line retreat. Once the grounding line is destabilized, it could continue to retreat in a self-enhancing fashion. How far the grounding-line retreats depends on multiple factors, including the geometry of the bed topography. For example, grounding lines in regions of retrograde bed slopes are expected to be especially susceptible to self-enhanced rapid retreat. This potentially irreversible process can be slowed or stopped by local factors, such as strong lateral or vertical shear stresses, brought about by the presence of pinning points or morphological landforms[79]. These landforms can be pre-existing tectonic features or formed through the deposition of subglacial and ice proximal sediments[79–82]. Rapid uplift of the bed owing to glacio-isostatic adjustment can further shoal those features and potentially slow down grounding-line retreat[83,84].

In the Amundsen Sea sector of West Antarctica, satellite-derived observations of pervasive grounding-line retreat since the 1990s[27,85,86] have raised concerns of the initiation of MISI. Indeed, some glaciers of the Amundsen Sea Sector, such as Pine Island and Thwaites glaciers, are prone to instability. These glaciers are probably not already engaged in irreversible retreat[87]; however, current climate conditions might be sufficient to eventually push these glaciers into a MISI[88]. MISI would destabilize the marine-based sectors of the AIS in the absence of sufficient ice shelf buttressing and other pre-conditioning factors[89–91].

In addition to MISI, another potential instability that could lead to rapid glacial retreat and amplify ice sheet mass loss is marine ice cliff instability (MICI)[92,93]. This mechanism would be triggered by the collapse of ice shelves, exposing an ice cliff at the grounding line. If the ice cliff is tall enough, the stresses at the cliff could exceed the strength of ice and the cliff could fail structurally, triggering repeated calving events[94]. Unlike MISI, MICI does not require a retrograde bed slope to occur and could also happen on a flat or prograde terrain. Furthermore, the percolation of meltwater into newly formed surface crevasses, alongside subsequent refreezing in situ, could further enlarge the crevasses and enhance MICI, leading to even faster rates of retreat[93]. Direct observations of cliff failure are, however, limited at present, making it difficult to assess whether MICI has ever occurred in the past. It is, therefore, challenging to accurately parameterize the retreat of marine-terminating glaciers that undergo cliff failure[95].

Short-term and long-term variability in Antarctic Ice Sheet mass balance

The drivers and processes of ice sheet mass change contribute to AIS variability across a range of timescales, including short-term fluctuations (sub-daily to decadal), long-term changes (multi-millennial) inferred from paleo-proxy evidence, and projected multi-decadal to multi-centennial changes (Fig. 3), as now discussed.

Short-term fluctuations

Most of the mass loss of the AIS since the 1990s has occurred in regions exhibiting strong basal melting, retreat, and thinning of ice shelves[27,42,43,45], implicating oceanic forcing as a key driver (Fig. 3b). Interannual to multi-decadal acceleration, thinning and retreat of Antarctic outlet glaciers[46–49] have been observed where warm waters from the depths of the Southern Ocean can upwell and be conveyed towards the base of ice shelves[29,42–44].

Over short timescales, tides induce hourly-to-daily variations in the amount of oceanic heat that is advected from the open ocean to the margins of the AIS[96,97]. Tides enhance the basal melting of ice shelves[98], explaining an estimated 4% of the AIS basal ice loss[99]. Satellite

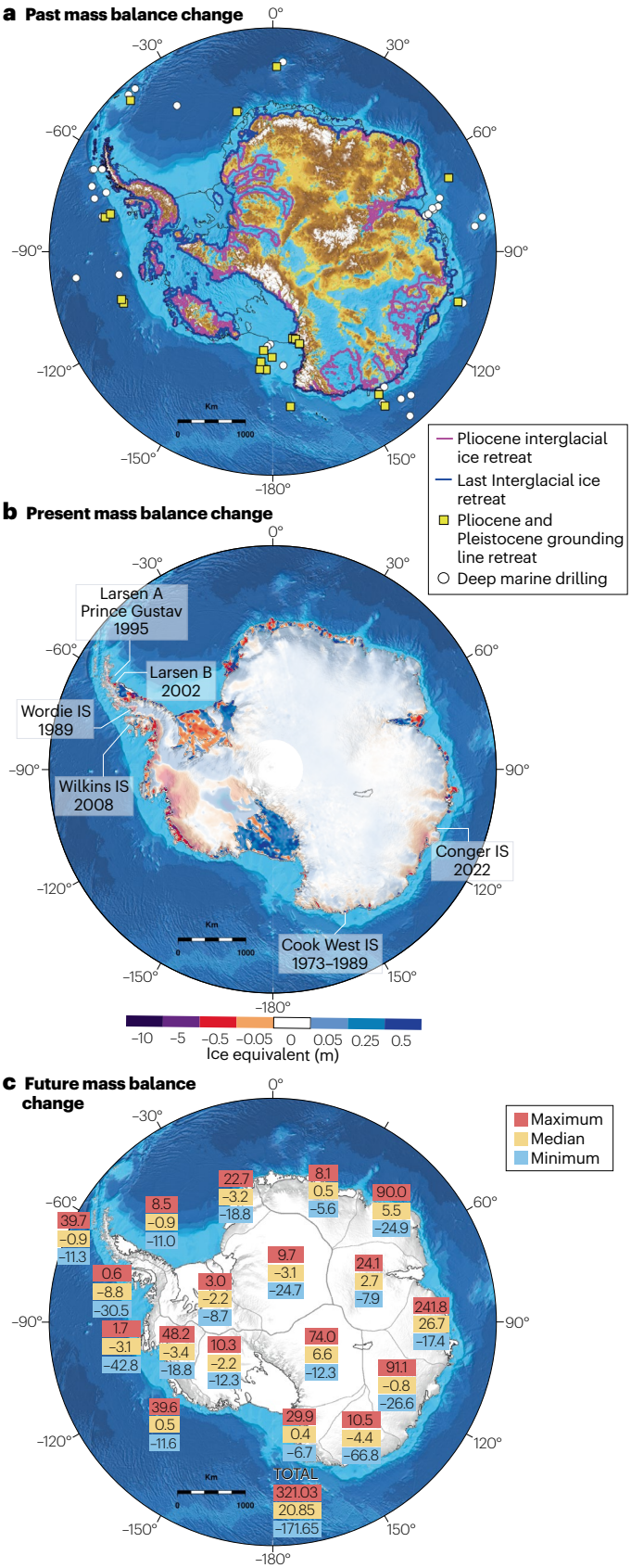

Fig. 3 | Past, present and future changes of the Antarctic Ice Sheet. **a**, Simulated Antarctic Ice Sheet retreat during a generic warm interglacial of the Pliocene (3.3–3.0 Ma, magenta line) and the Last Interglacial (~130 ka, blue line) accounting for marine ice cliff instability[94]. White circles indicate deep marine sediment drilling sites (Deep Sea Drilling Project, Ocean Drilling Program, International Ocean Discovery Program), and yellow squares mark sites that provide geological evidence for grounding-line retreat during the Pliocene and Pleistocene epochs[254]. **b**, Observed Antarctic ice thickness changes from 2003 to 2019 (ref. 42) and locations of ice shelf (IS) collapse. Grounded ice thickness change is semi-transparent to emphasize rates of ice shelf thinning. **c**, Ice Sheet Model Intercomparison Project 6 ensemble member-derived[141] estimates of maximum (orange), median (yellow) and minimum (blue) volume changes above floatation (in millimetres) by 2100 under representative concentration pathway 8.5 for individual drainage basins[27]; changes are calculated relative to 2015 using 362.5 Gt = 1 mm sea level rise as a standard conversion factor[63]. Positive values indicate a contribution to global mean sea level rise. In parts **a** and **c**, the black line corresponds to the present-day grounding line and coastline from BedMachine Antarctic v3 (ref. 225). In **a**, **b** and **c** bathymetry is from IBCSO v2 (ref. 255). Knowledge of the past and ongoing behaviour of the Antarctic Ice Sheet is essential for accurately constraining projections of its future evolution. ka, thousand years ago; Ma, million years ago.

interferometry has revealed that tides also cause short-term fluctuations in the grounding-line position ranging from a few kilometres to over 15 km (refs. 27,85). Such behaviour allows oceanic water to penetrate to the grounding zone and beyond, increasing oceanic-enabled melting[100,101].

Atmospheric forcings through processes such as atmospheric rivers, accumulation, melt events[102] or other extreme weather events can also induce strong short-term variability in the AIS surface mass balance. Such events are regionally linked to large-scale modes of atmospheric–ocean circulation variability, especially El Niño Southern Oscillation-related tropical Pacific warm episodes and the increasingly positive Southern Annular Mode. The Amundsen Sea Low atmospheric pressure system modulates the links between larger-scale teleconnections of the AIS' surface mass balance[13].

Basal melting in the AIS exhibits interannual variability. Across Antarctica, this variability is linked to the effects of oceanic forcing including tropical Pacific atmosphere–ocean teleconnections, the southward shift and intensification of the westerly winds offshore from Antarctica (which regulate the upwelling and advection of Circumpolar Deep Water (CDW) towards the continent[29,103–105]), intrinsic oceanic variability[106], and a remote connection with the variability of the Amundsen Sea Low[107]. For ice sheets in quasi-equilibrium with the climate, these interannual variations in oceanic forcing are not expected to cause substantial deviations from the equilibrium state. Indeed, high basal melt rates (>10 m year^{-1}) do not necessarily imply that the ice shelves and tributary glaciers are out of balance. However, a sustained climate anomaly or long-term trend in oceanic forcing could perturb the system to a new stable state.

The direct influence of surface melting on AIS mass loss is negligible at present[42], and the ice shelves of Antarctica have only experienced minor changes in surface melt since 1980 (ref. 69). However, the contribution of melt to the overall mass imbalance of the AIS is expected to increase with climatic warming[61,65]. Atmospheric warming over the Larsen B Ice Shelf since the Holocene[108] provides a good analogue for the potential implications of such warming for Antarctica's ice shelves more generally. Such warming made Larsen B vulnerable

to the presence of liquid water at its surface. Prior to its 2002 collapse, the ice shelf had experienced two decades of progressive surface lake expansion coinciding with regional climatic warming of approximately 2.5 °C during the mid-late twentieth century[109]. The collapse coincided with the drainage of over 2,000 surface lakes, which are suggested to have contributed to the break-up event through ice shelf flexing, weakening and fracturing[110–112]. The rapid disintegration of Larsen B instigated prolific inland glacier acceleration owing to the loss of buttressing after the collapse of the ice shelf[74,113]. Similar mechanisms, together with enhanced, ocean-driven basal melting, have also been implicated in the break-up of Wilkins Ice Shelf in 2008 (ref. 5). Ultimately, the fate of both ice shelves underscores how sustained extreme warm weather events associated with atmospheric river activity, alongside ocean swell wave-induced damage, have the potential to trigger ice shelf disintegration[11,60,67,114,115].

As for the GrIS, surface melt on the AIS percolating under grounded ice might also increase ice discharge. For example, the rapid (~15–100%) intra-annual acceleration of multiple glaciers in the Antarctic Peninsula could be controlled by surface meltwater inputs to the subglacial environment[76,77]. Additionally, glacier velocity and geometry measurements suggest that changes in surface climate (such as temperature) and, therefore, melt rates might directly influence active subglacial hydrological networks in the region[77,116].

Finally, the discharge from the AIS of icebergs and meltwater in the upper ocean layers could temporarily cause an expansion in sea ice cover[117]. This expansion warms subsurface waters through enhanced water mass stratification and lowers near-surface air temperatures around the Antarctic margin[118,119]. This phenomenon also traps warm CDW in intermediate ocean layers, funnelling it towards the undersides of the ice shelves of Antarctica wherein melting is maximized near the grounding line[118–120]. The resulting amplifying feedback from ice loss caused by increased sub-ice shelf melt, and the damping feedback caused by atmospheric cooling, could therefore be important for the long-term future of the AIS[92].

Reconstructed long-term changes

The far-field geological record indicates that, during the past periods of warm climate, sea levels were higher than at present, implying that partial melting of the GrIS and AIS occurred in those time intervals. Sea level was more than 7 m higher than at present in the mid-Pliocene Warm Period (3.3–3.0 million years ago (Ma)), during which, the atmospheric CO_2 levels peaked above 400 ppm (refs. 121,122), which is broadly similar to today's CO_2 levels. During the early-Pleistocene, mid-Pleistocene and late-Pleistocene Marine Isotope Stages (MIS; MIS 31 (1.1–1.0 Ma), MIS 11c (426–396 thousand years ago (ka)) and MIS 5e (128–116 ka), respectively), atmospheric CO_2 levels were around 300 ppm or less and the ocean–continent configuration was similar to that of today but the Southern Hemisphere surface temperature exceeded that of today owing to astronomical forcing.

Geological archives in the Antarctic interior and margins yield proxies for precipitation, temperature, sea ice, salinity, water depth and circulation during the past interglacials[123], which can be used to reduce uncertainties in the absolute values of the contributions of the AIS and GrIS to the past sea level change. These data document ice margin retreat of up to several hundred kilometres in the Ross Sea and in the Wilkes Subglacial Basin (WSB), East Antarctica, during the warm Pliocene[124,125] and late Pleistocene interglacial intervals[126], when Antarctic air temperatures were at least 2 °C higher than pre-industrial levels for ≥2,500 years (Fig. 3a). Numerical simulations constrained by ice and sediment cores show that the ice could have retreated by approximately 100–330 km from the WSB around 330,000 and 125,000 ka, coinciding with periods of warmer Southern Ocean conditions and a global mean sea level that was 4–6 m higher than that at present[127] (Fig. 3a). If paleo and modern oceanographic data, which are still lacking for the Antarctic continental margin, provide information about present conditions and confirm these simulations, these findings suggest that even modest (~0.5 °C) future warming would be sufficient to cause ice loss from the WSB[128].

Elsewhere in Antarctica, marine geomorphological evidence has revealed that the grounding line of the Ross Sea continental shelf region receded 200 km from the shelf edge over several centuries during the last deglaciation (~11.5 ka) (ref. 80). During this time, similar styles of rapid retreat also occurred across the Marguerite Bay region offshore of the Antarctic Peninsula[79]. Although proxies can help to establish ice sheet sensitivity to external climatic forcing, they can only be used to approximate a low temporal or spatial resolution climate average state. Therefore, numerical modelling is needed to assess the importance of nonlinear variability for AIS processes.

Projected long-term changes

Projected global warming of approximately 5 °C over Antarctica by 2100 under continued strong anthropogenic greenhouse warming[129] could result in substantial surface melt over large areas of the AIS. For example, runoff is estimated to increase as a fraction of surface mass balance from the current 1.5% to >7% by the 2090s (ref. 130). The resulting mass loss from increased melting is projected to be partly compensated by increases in Antarctic snowfall by 2100, although considerable uncertainty about the magnitude of this offset remains[63,64,130,131]. Therefore, whether or not the surface melt caused by atmospheric warming could contribute to the disintegration of an entire glacial basin on centennial to millennial timescales is unclear[94].

Future climate warming will also increase the supply of oceanic heat to ice shelf cavities. In cavities that are currently exposed to frequent warm CDW intrusions in the Amundsen Sea[132] and some parts of East Antarctica[133], this oceanic heat could lead to enhanced basal melt and exacerbate sea level rise (Fig. 3c). Other, currently cold, ocean cavities with no or seldom CDW intrusions, for example, the cavity on the Filchner–Ronne Ice Shelf[134–136], could transition to warm cavities under high greenhouse gas emission scenarios. Such transitions could have important implications for the mass balance of adjoining ice streams and neighbouring ice sheet drainage areas (Fig. 3c).

Increases in ocean-driven basal melting, surface ablation or calving rates could lead to widespread ice stream grounding-line retreat[27,93,137–140]. The grounding lines of the large Thwaites and Pine Island glaciers in the AIS have already retreated by more than 1 km $year^{-1}$ since the 1990s (refs. 85,86). Several glacier and ice sheet and shelf models suggest that these grounding lines could retreat far inland (tens of kilometres or more) of their present-day position in the future[90,92,141], as they did during the mid-Pliocene Warm Period and/or some of the Pleistocene warm interglacials (Fig. 3a).

At the continental scale, current ice sheet models predict that the AIS will contribute 3–32 cm to sea level rise (relative to the 1995–2014 baseline) by 2100 in the case of the high-emission Shared Socioeconomic Pathway (SSP) 5–8.5 (>1,000 ppm atmospheric CO_2)[3] (Fig. 3c). For a Paris Climate Agreement-like future scenario or better (low-emission scenario SSP1–2.6, <450 ppm atmospheric CO_2), the contribution of the AIS to sea level rise by 2100 is similar to that of SSP5–8.5 (3–27 cm)[3].

MICI could increase the future mass loss of Antarctica in high-emission scenarios. Indeed, including an explicit parameterization for MICI under SSP5–8.5 increases the projected contribution of the AIS to sea level rise by 2100 to 2–56 cm, but this estimate is uncertain and only based on one model[92]. Under low-emission SSP1–2.6 scenarios that account for the contributions of MICI, the projected contributions of the AIS to sea level rise by 2100 are again similar to those of SSP5–8.5 (ref. 3).

However, over much longer (multi-centennial) timescales, the difference between the sea level rise projected by the two SSP scenarios clearly emerges. Under SSP1–2.6, the contribution of AIS to sea level rise is up to 78 cm and could reach 135 cm by 2300 if parameterizing for MICI[3]. However, under SSP5–8.5 scenarios, the projected AIS contribution reaches 3.13 m and increases to over 13 m if MICI is accounted for[3]. Uncertainties related to the knowledge gaps about MICI and ice–ocean interactions currently preclude more accurate projections of the future contribution of AIS to sea level. However, the estimated multi-metre sea level rise falls within the range inferred from geological records for key warm paleo periods[121,122] (Fig. 3).

Interaction of short-term and long-term changes

Most short-term atmospheric and oceanic fluctuations around Antarctica, which cause episodic calving or anomalous snowfall or melt events, are linked to the internal variability of the climate system. The AIS is not currently in steady state; therefore, short-term variations in atmospheric or oceanic conditions can trigger self-reinforcing (amplifying) feedbacks that increase the sensitivity of the AIS to longer-term climatic forcing. For example, observations of ice flow in the Amundsen Sea Embayment or the collapse of Larsen B Ice Shelf illustrate that variability in ocean-induced and atmosphere-induced melting can trigger ice thinning, retreat or collapse of ice shelves, grounding-line retreat and ice flow acceleration.

The trigger mechanism for these rapid, MISI-like grounding-line migration events has been ascribed to the impact of an array of intermittent, atmosphere-related and ocean-related forcing events on the Antarctic coastal margin[80,142,143]. The retreat observed in the Amundsen Sector since the 1990s is associated with a multi-decadal trend in climatic forcing over at least the past 100 years (ref. 144), although internal climate variability also has an important contribution[145].

The marine geomorphological record[81,82,146] has revealed that pulses of extremely rapid grounding-line retreat (between 10 and 600 m day^{-1}) can occur at tidal (sub-daily to daily) timescales in the absence of the steeply retrograde bed topography that is conducive to MISI. These pulses of retreat are only sustained for periods of days to months; thus, this behaviour could represent an example of ice sheet perturbation in response to short-term, weather-type forcing. Offshore of the Antarctic Peninsula, marine geomorphological data reveal that a grounding-line retreat rate of up to 50 m day^{-1} (equivalent to ≥10 km year^{-1}) occurred during regional deglaciation of the continental shelf (approximately 10.7 ka) (refs. 79,81,82). This constitutes the highest rate of retreat recorded in Antarctica so far. However, grounding-line retreat rates near this magnitude have recently been detected in West Antarctica by satellites (~30 m day^{-1} over the course of 3.6 months in 2017 at Pope Glacier[138]), offering important corroboration of these past magnitudes of retreat.

Marine geomorphological observations also reveal the highly nonlinear nature of ice sheet retreat, with substantial pulses of grounding-line retreat occurring over short timescales punctuated by longer periods of relative stability. Furthermore, they highlight the important role of ice sheet bed geometry in modulating the rate of retreat, by showing that flat-bedded parts of ice sheets are particularly vulnerable to pulses of rapid ungrounding[146]. The long-term ice dynamical response of the AIS to such rapid recession remains unknown. Nonetheless, the prolific rates of retreat inferred from these records imply that, even in the absence of MISI and MICI, the future pace of short-term AIS retreat over such vulnerable regions could be substantially greater than most satellite-derived and model-derived insights suggest.

Short-term and long-term variability in Greenland Ice Sheet mass balance

The mass balance of the GrIS also changes over various timescales, including short-term fluctuations (sub-daily to interannual), observed long-term changes (decadal to geological) and projected decadal to centennial changes, as outlined here.

Short-term fluctuations

Short-term fluctuations in the GrIS mass balance mainly arise from surface melting. Extreme examples linked to climate warming are the record seasonal melt events in the summers of 2012 and 2019 (ref. 147), when over a few days to a few weeks, approximately 60–90% of the surface temporarily melted: a phenomenon that has not been seen since at least 1979 (the start of the satellite record). The 2019 melt event resulted in a record of 444 Gt year^{-1} mass loss, which is approximately double the average mass loss for the 2010s (ref. 148) (Fig. 1). Additionally, in September 2022, an unprecedentedly late seasonal melt occurred, involving 36% of the ice sheet surface including the Summit station at an elevation of 3,250 m (ref. 149). Surface meltwater can infiltrate to the bed and increase ice flow. The ice dynamical response to surface melting can occur on diurnal to weekly timescales[150–152], depending on the amount of melt and the seasonally evolving subglacial drainage efficiency. In summer, the peak ice flow speeds often exceed the annual mean by 25–100% in the fast-flowing areas 40 km inland from the GrIS margin[150,153–155].

Extreme melting is often driven by atmospheric blocking and is also associated with the delivery of heat and moisture by atmospheric rivers[10–12]. The frequency of the incursion of moisture-laden air masses has increased by >6% between 1979 and 2015 (ref. 156). During an atmospheric river episode in mid-August 2021, rainfall occurred at Summit station, apparently for the first time in modern history, prolonging melt conditions through the ensuing melt–albedo feedback[14]. With Greenland climate warming[157], the melt threshold in the lower atmosphere is more frequently crossed; therefore, rainfall constitutes an increasing fraction of the total precipitation[158] (Fig. 4).

Tidewater glacier calving enables large-scale mass loss to occur over short timescales. Calving-induced changes in near-terminus stresses can disrupt upstream ice flow on timescales of minutes[159] to days[160,161]. Changes in the frontal position of tidewater glaciers driven by variation in submarine melting and/or calving rates can trigger increases in dynamic mass loss that last several years and have a marked impact on regional mass balance[162]. Observations and modelling suggest that short-term surface meltwater variability affects the calving dynamics of Greenland tidewater glaciers[38,163,164] but the net effect is complicated by the effect of the stress state at the glacier terminus, which can be modified by bed topography[165,166], tidal variation[167,168], submarine melt[169,170], surface meltwater ejection from the grounding line into fjord waters[163] and the stabilizing effect of sea ice and mélange[171,172].

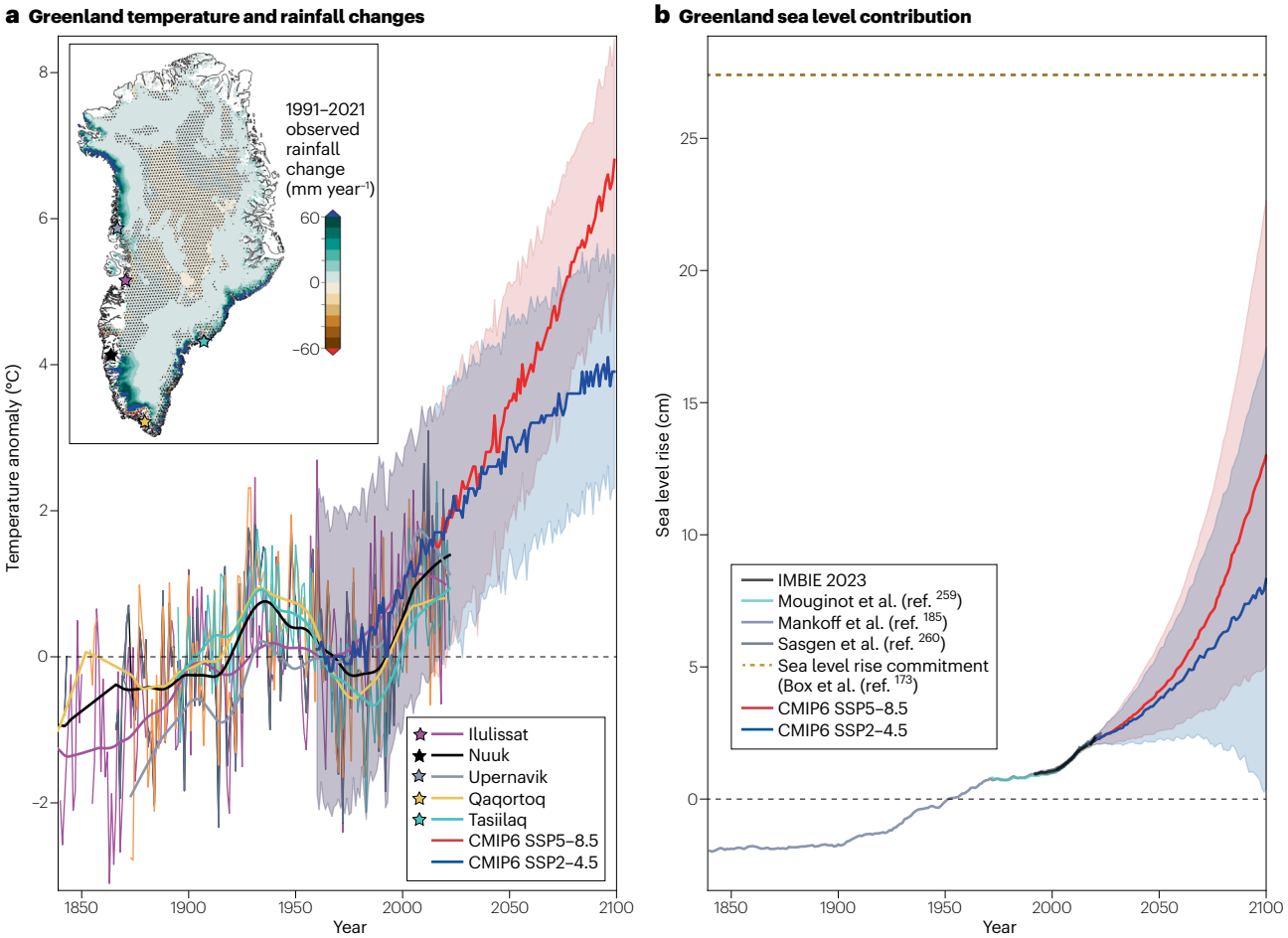

Fig. 4 | Past and future Greenland air temperature and sea level contribution between 1850 and 2100. a, Observed and projected June through August summer air temperatures. The observed temperatures are from land-based stations at Ilulissat, Nuuk, Upernavik, Qaqortoq and Tasiilaq (updated from ref. 256) (stars on the inset map, with corresponding line colours), and the projected temperatures include the ensemble mean of CMIP6 models forced with SSP2–4.5 (blue) and SSP5–8.5 (red)[257]; shading represents one standard deviation of the ensemble. The inset depicts Copernicus Arctic Regional Reanalysis-derived[258] rainfall trends over 1991 to 2021, with non-stippled areas indicating trend confidence above 66% measured using 1 minus the *p*-statistic, suggesting statistically significant difference from a random series. **b**, Greenland Ice Sheet contributions to sea level, with observations[148,185,259,260] offset to align with CMIP6 SSP5–8.5 (red) and SSP2–4.5 (blue) projections[257], which start in 2016; shading represents one standard deviation of the ensemble. The Sasgen et al. mass balance data are only visible for the last 2 years[260]. The brown dashed line indicates the level of ice sheet loss committed throughout 2000–2019 (ref. 173). Greenland Ice Sheet contributions to sea level have started to depart from a period of relative stability. CMIP6, Coupled Model Intercomparison Project Phase 6; SSP, Shared Socioeconomic Pathway.

Observed long-term changes

Over 2002–2020, the average mass change of the GrIS was −235 ± 21 Gt year^{-1} (ref. 148). During 2007–2017, the overall mass loss was estimated to comprise a 64% contribution from surface mass balance and 36% from ice dynamical losses, with the largest rates of GrIS surface elevation change (in excess of −1 m year^{-1}) occurring at fast-flowing marine outlets[68]. It has been suggested that the surface ablation through meltwater runoff could be the primary control on the trend and interannual variability of the GrIS mass budget[173].

Elevation changes in Greenland are driven by various competing processes. Satellite altimetry revealed a slight increase (~0.1 m year^{-1}) in surface elevation in the interior GrIS above 2,000 m elevation between 2007 and 2017, suggesting that snow accumulation increased during this period of increasing temperatures[68]. However, surface mass balance models generally underestimate snow accumulation in the interior GrIS[174] and cannot explain the observed interior thickening[68]. Greenland atmospheric warming[157] has been accompanied by melt, runoff and rainfall increases[158,175] that have outpaced the 7% increase in snowfall accumulation per degree Celsius warming during 1840–1999 (ref. 176). In the snow accumulation area, increased refreezing in the firn has led to an expansion of partly impermeable ice slabs by 26 ± 3% since 2001, limiting firn meltwater storage and enhancing lateral runoff through firn[177,178]. This deterioration of the firn layer includes an expansion of the bare ice area by approximately 20–34% during 1958–2017 across the GrIS[20,179,180]. Firn deterioration is further augmented by melt and rainwater storage in perennial firn aquifers, and in the south-east of the GrIS, aquifer area has increased[181].

However, ice core paleoclimatic reconstructions indicate that the GrIS is more resilient than what regional climate model (RCM) projections suggest, with temperatures 8 ± 4 °C above the mean of the past millennium[182] producing a modest ~2 m sea level rise during the previous interglacial, the Eemian (130–115 ka). Additionally, throughout the last 11,700 years of the current interglacial, an initial thinning of several hundred metres occurred in the northwest and southeast of GrIS during the first few thousand years after the glacial–interglacial transition. The interior areas have since remained stable within a few hundred metres throughout the Holocene[183].

Projected long-term changes

The contributions of the GrIS to sea level rise vary under the different emission scenarios. For the SSP5–8.5 high-emission scenario, GrIS model projections from the Intergovernmental Panel on Climate Change's (IPCC's) Sixth Assessment Report (AR6)[3,63,131] yield a 13 cm (with a probable range of 9–18 cm) contribution to sea level rise by 2100. Under a Paris Climate Agreement-like future scenario (SSP2–4.5), the sea level rise contribution is 8 cm (probable range of 4–14 cm), which is 62% of the high-emission amount. The two scenarios increasingly diverge after 2050, with summer air temperatures over Greenland differing by 0.6 °C by 2050 and 2.4 °C by 2100 (Fig. 4).

The two decades (2002–2022) of observed GrIS mass change[184] (Fig. 1) indicate an average sea level rise contribution of 0.70 ± 0.05 mm year^{-1}. Analysis of different satellite data and regional climate modelling yields a similar rate (0.61 ± 0.25 mm year^{-1}) over the same period[185]. These two 20-year rates are not reached by the median estimate of the AR6 projections in the SSP2–4.5 scenario until some two to three decades later (Fig. 4): 2029–2049 (ref. 184) and 2022–2042 (ref. 185), respectively. Under the SSP5–8.5 (ref. 3) scenario, these rates are reached by 2021–2041 (ref. 185). The differences between observed and projected mass balance changes are, however, within the error envelope of the AR6 projections. The differences probably arise from a combination of the limitations of the global climate model (GCM) and RCM forcing (for example, using an inaccurate representation of atmospheric circulation changes), the wide range of Ice Sheet Model Intercomparison Project 6 (ISMIP6) model results[63], and observed processes not being fully incorporated into ice sheet model projections.

Currently, models simulate that about half of the surface meltwater on the GrIS is refrozen and retained in the firn[186]. Under future warming scenarios, the ability of the firn to retain meltwater could decrease and eventually be lost, and centuries of cold climate would be required for this ability to be regained. Climate projections under the high-emission scenario SSP5–8.5 show that the refreezing capability could start to permanently decline by 2100 (ref. 187).

Additionally, RCMs project that a warming climate will lead to increased precipitation over Greenland; however, the amount of future increase in snow accumulation is uncertain. Projected surface mass balance suggests that surface melt and runoff will far outweigh any increase in accumulation[188–190]. Climate warming has also contributed to increased GrIS snow line altitudes and a mass budget deficit. If the average deficit realized over 2000–2019 remained constant, it would lead to a contribution to sea level rise of at least 27 ± 7 cm (ref. 173). Modelling suggests that the GrIS adjusts to surface mass balance perturbations across annual to multi-millennial timescales[191–193].

Interaction of short-term and long-term changes

Short-term and long-term GrIS changes and their interactions are modulated by climate variability as a key influence on mass balance. Extreme atmospheric blocking episodes led to near-record surface meltwater runoff from the GrIS in 2012 and 2019 (ref. 147). However, these record atmospheric events were either followed (2013) or preceded (2018) by low melt anomalies, highlighting the impact of increased interannual variability on extreme glaciological events and ice sheet evolution.

The response of tidewater glaciers to atmospheric and oceanic forcing remains a key uncertainty when projecting future mass loss from the GrIS[3]. This uncertainty arises owing to seasonal ice velocity fluctuations at tidewater glaciers, which are influenced by surface melt and runoff, subglacial hydrology and ice–ocean interactions at the ice front[155]. This variability is a complex response to surface meltwater, basal drainage, calving events and break-up of mélange at the tidewater terminus[153,194]. For example, atmospheric circulation anomalies during 1995–1996 drove a warm ocean current, which destabilized the largest tidewater glacier in the west GrIS[195] and increased the meltwater runoff, leading to underwater melting[36]. However, interannual flow variability can also be a response to both contemporary terminus retreat or a lagged response to inland changes in snowfall and ice flux[196–198].

As the infiltration of surface meltwater increases, the extent to which the lubricating effects of melt on glacier flow are self-regulating, and therefore affect the short-term and long-term variability of the hydrology and dynamics of the GrIS, remains a key topic. Global Navigation Satellite System (GNSS) and surface climate measurements in western Greenland[150] confirm that there is an annual ice flow cycle, which is coupled to surface meltwater production and transport into the subglacial drainage system[199]. Ice acceleration decreases as the melt season progresses, indicating the development of an efficient, lower-pressure subglacial drainage network[200]. Although this self-regulation has now been firmly documented[201,202], it has not been observed more than 40 km inland from the GrIS margin. The efficiency of meltwater routing and subglacial drainage tends to increase with climate warming and limit the impact of runoff fluctuations on annual ice flow velocities or multi-annual acceleration[62,154,194,203]. This limited impact contrasts with the much clearer effect of runoff fluctuations on diurnal to seasonal-scale flow[151–153].

Inland and up to 140 km from the ice margin, where thicker ice and lower surface melt rates occur, persistent ice flow acceleration has been observed in winter and summer at and above the equilibrium line[204]. The underlying cause of this acceleration appears to be the upstream migration of distributed subglacial drainage along with the potential for viscous warming and decoupling of a previously frozen bed. The area over which such meltwater penetration occurs is projected to increase under future climate scenarios[205]. Late melt season rainfall is also thought to contribute to the acceleration of land-terminating glaciers[206]. However, the relatively modest net values of ice acceleration observed across the equilibrium line (~1 m year^{-1} over a period of 3 years (ref. 204)) means that it is unlikely to substantially influence mass loss relative to changes in surface mass balance or the major dynamic changes documented at tidewater glaciers[207].

The many scales of iceberg calving, from the day-to-day crumbling of small bergs to the detachment of large tabular bergs at intervals of years to decades[208], are a continuum connecting the short-term and long-term dynamics of marine outlet glaciers. Sustained retreats of calving termini often co-occur with dynamic drawdown of ice from tens of kilometres upstream[209,210]. Numerical models suggest that temporal disturbances of calving termini can initiate long-term, large-scale dynamic changes far into the ice sheet interior[211]. Glacier outlet geometry, including the ice thickness and the presence or absence of steep knickpoints in the bed topography, controls how fast and how far a wave of thinning

initiated at the terminus can propagate inland[212]. High-melt years, or consecutive years with high melt and loss of mélange, can destabilize the terminus and trigger a rapid dynamical retreat[213]. Glacier sensitivity to terminus position could depend on tides[167] and near-terminus bed topography. Therefore, when the terminus is near a susceptible point in the bed, normal calving could initiate multi-annual retreat[160,214]. Ice sheet models show that failing to account for seasonal-scale to decadal-scale climate variability of marine-terminating glaciers can bias the projected multi-decadal mass loss[215,216].

Summary and future perspectives

Ice sheet mass change is driven by various processes including atmospheric and oceanic forcing and sea ice and hydrological changes. Such processes induce changes in ice sheets on timescales ranging from days to centuries and can, therefore, introduce substantial uncertainty into ice sheet model projections. The short-term and long-term variability in the AIS and GrIS can be revealed through observations, models and reconstructions from geological records, giving insight into how these changes interact with one another. Despite this knowledge, continued and enhanced monitoring and modelling efforts are required to fully partition the relative importance of short-term and long-term effects in driving future ice sheet demise. Such efforts should focus on understanding high-resolution mass changes; high-elevation, tidewater glacier and ice shelf hydrology and dynamics; calving; ocean heat flux; and grounding zone bed geometry, to more accurately predict the future evolution and contribution to sea level of the GrIS and AIS.

Satellite monitoring

Upcoming spaceborne observation systems such as NISAR (a NASA–Indian Space Research Organization Synthetic Aperture Radar mission), which will launch in 2024, and the European Space Agency (ESA)'s Harmony mission, which will launch in 2029, will further extend understanding of short-term changes across the polar regions. Both missions will have extensive capabilities to sample the deformation (flow dynamics and grounding-line migration) of ice sheets at weekly resolution with unprecedented precision. These data should be used to interpret and constrain models, provide feedback to the missions, and help design the next generation of polar orbiting satellite sensors.

Since 2002, the Gravity Recovery and Climate Experiment (GRACE) mission led by NASA and the DLR (Deutsches Zentrum für Luft-und Raumfahrt, German Aerospace Center) and its successor, GRACE-Follow-On (GRACE-FO), have provided accurate, spatially comprehensive and continuous assessment of mass change across the ice sheets[217] (Fig. 1). The data from these missions are needed to constrain models and projections of sea level rise. A GRACE-FO successor mission led by GFZ (Deutsches GeoForschungsZentrum, German Research Centre for Geosciences)–DLR and NASA–JPL (Jet Propulsion Laboratory) is scheduled for launch in 2027. This mission will fly an upgraded laser-ranging interferometer, which will improve intra-satellite distance measurements by two orders of magnitude[216], leading to corresponding enhancements in the spatial and temporal resolution of mass change observations[218,219]. In parallel, the ESA Ministerial Council is working to launch an additional GRACE-FO-type satellite pair in 2031. The Mass change And Geosciences International Constellation (MAGIC)[220], comprising both GFZ/DLR–NASA/JPL and ESA satellite pairs, will reduce and homogenize uncertainties of global sea level change estimates. Beyond these missions, continued international investment into initiatives such as the EU Copernicus programme and the long-running NASA–US Geological Survey (USGS) Landsat programme will be key to ensuring the long-term ability to routinely monitor the ice sheets from space.

Aside from the (multi-)national, space agency-managed Earth observation programmes mentioned above, an increasing number of commercial companies have launched dedicated, ultra-high-resolution imaging satellites capable of providing daily to sub-daily optical- and radar-based observations of ice sheet change (including ice shelf rifting, fracturing and iceberg calving) with ~1 m spatial resolution or better. This high resolution enables such data to offer insights that might not be possible from conventional imaging afforded by the Landsat and EU Copernicus–ESA Sentinel constellation of satellites. Despite these opportunities, most commercial satellite imagery presently comes with substantial cost, usage restrictions and/or other access barriers at the ice sheet scale. We therefore advocate for increased dialogue with these companies to encourage dedicated and routine commercial satellite image acquisition over the polar regions and open-access use by the international scientific community. Upcoming initiatives such as the International Polar Year 2032–2033 can and should act as important catalysts for such dialogue.

In situ observations

In situ observational data are urgently needed to improve understanding of ocean conditions offshore of Greenland and Antarctica and of sub-ice shelf conditions. Autonomous Argo floaters (floating devices that drift with the ocean currents and periodically move up and down with a depth range of ~2,000 m, taking measurements of temperature and salinity) are now ready to operate in ice environments and should be immediately deployed to provide a comprehensive observational network across the polar oceans. Additionally, the Argo-derived observations should be complemented by measurements from MEOP (marine mammals exploring the oceans pole to pole) conductivity, temperature and depth probes deployed on sea mammals and observations of the ice sheet proximal environment collected using robotic devices[221,222] and other in situ techniques[223]. Such an observational network would provide sufficient data to enable models to constrain ocean state and ice melt rates at the ice sheet margins with minimized uncertainty. In Antarctica, this observation network should ideally extend to the grounding zone because this region is crucial to ice sheet evolution, is difficult to access, and is poorly observed at present. In Greenland, the difficulty of obtaining in situ measurements of submarine melt rate severely limits understanding of the importance of this process at tidewater glaciers. Dedicated field campaigns[224] and new technologies and methodologies are needed to address this deficiency.

Knowledge gaps about the Antarctic subglacial topography, especially around grounding zones[225] and on the continental shelf[226] (Fig. 3a) under areas of present-day ice shelf cover, currently preclude understanding of ice sheet dynamics in response to atmospheric and oceanic forcing in sectors that are potentially vulnerable to rapid retreat. It is, therefore, important that the understanding of the precise geometry and geological composition of the AIS grounding zone at the continental scale is improved through dedicated in situ geophysical campaigns such as that proposed by the Scientific Committee on Antarctic Research (SCAR)-funded RINGS and IBCSO (International Bathymetric Chart of the Southern Ocean) groups. Seaward of the present-day grounding zone, systematic bathymetric and sub-seafloor measurements over deglaciated margins are expected to yield important insight into the configuration and behaviour of past and present ice sheets[81,82,146], with additional importance for setting boundaries and validating and reducing uncertainty in models.

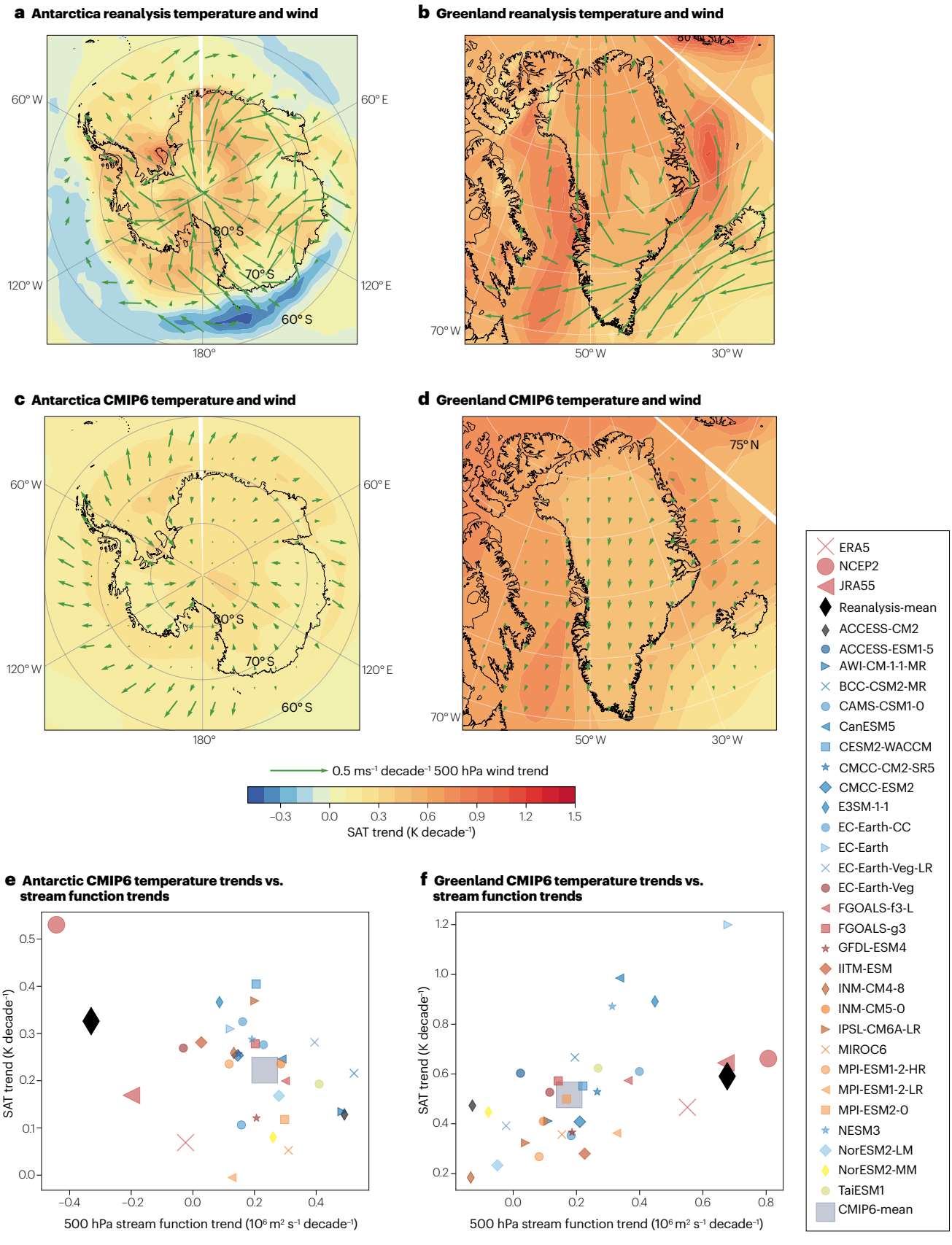
a Antarctica reanalysis temperature and wind
60° W
60° E
120° W
120° E
180°
80° S
70° S
60° S
b Greenland reanalysis temperature and wind
70° W
50° W
30° W
c Antarctica CMIP6 temperature and wind
d Greenland CMIP6 temperature and wind
75° N
0.5 ms⁻¹ decade⁻¹ 500 hPa wind trend
−0.3
0.0
0.3
0.6
0.9
1.2
1.5
SAT trend (K decade⁻¹)
e Antarctic CMIP6 temperature trends vs. stream function trends
f Greenland CMIP6 temperature trends vs. stream function trends
SAT trend (K decade⁻¹)
500 hPa stream function trend (10⁶ m² s⁻¹ decade⁻¹)
ERA5
NCEP2
JRA55
Reanalysis-mean
ACCESS-CM2
ACCESS-ESM1-5
AWI-CM-1-1-MR
BCC-CSM2-MR
CAMS-CSM1-0
CanESM5
CESM2-WACCM
CMCC-CM2-SR5
CMCC-ESM2
E3SM-1-1
EC-Earth-CC
EC-Earth
EC-Earth-Veg-LR
EC-Earth-Veg
FGOALS-f3-L
FGOALS-g3
GFDL-ESM4
IITM-ESM
INM-CM4-8
INM-CM5-0
IPSL-CM6A-LR
MIROC6
MPI-ESM1-2-HR
MPI-ESM1-2-LR
MPI-ESM2-0
NESM3
NorESM2-LM
NorESM2-MM
TaiESM1
CMIP6-mean

Fig. 5 | Atmospheric circulation and associated surface temperature changes. a, Annual mean surface air temperature (SAT, colour bar) and wind trends (green arrows, 500 hPa zonal or meridional wind trends) over 1979–2020 in the mean of four reanalyses (ERA5 (ref. 261), NCEP2 (ref. 262), JRA55 (ref. 263) and MERRA2 (ref. 264) in Antarctica. **b**, As in **a**, but for Greenland. **c**, SAT and wind trends in Antarctica over 1979–2020 from the mean of 29 CMIP6 global climate models[257]. **d**, As in **c**, but for Greenland. **e**, SAT and 500 hPa stream function (rotational component of winds) trends in individual reanalyses[261–264] and CMIP6 models[257] for West Antarctica (60–90° S, 0–180° W; only land points) following ref. 237. **f**, As in **e**, but for Greenland (also only land points). Winds are poorly represented by the global climate models for the Greenland Ice Sheet, and SAT and winds are poorly represented for the Antarctica Ice Sheet. CMIP6, Coupled Model Intercomparison Project Phase 6.

A similar (and substantially increased) network of surface-based energy balance-enabled weather stations with radiation sensors will be needed to improve model-based and satellite-based estimates of AIS surface melt and firn hydrology. A similar effort on the GrIS under the guidance of the Geological Survey of Denmark and Greenland has led to excellent ice sheet wide coverage from around 2010, enabling the calibration of satellite-based surface melt rate estimates using machine learning techniques[227]. Additional arrays of in situ observations are required to improve model representations of ice shelf flexure and hydrofracture in response to surface meltwater ponding and drainage. Valuable observations could include water pressure measurements to monitor lake depths, arrays of GNSS stations to quantify ice shelf flexure[228], and seismic data to give insights into fracturing and rifting.

Ice sheet modelling

A major challenge for the modelling community is capturing the long-term ice sheet dynamics trend occurring at the continental to global scale and the short-term response occurring at local to regional scales within the same simulation. More sophisticated ice sheet models — constrained directly using knowledge from satellites, marine geomorphological records and in situ field observations — are needed to better predict future trends of rapid ice sheet evolution. Observationally constrained, regional-scale process models[151,228] have yet to be upscaled to the ice sheet scale, underscoring the need for comprehensive in situ observations to improve model-based predictions of the rate at which the ice sheets will respond to long-term and short-term forcing.

There are various processes that current models do not explicitly simulate, including decreased permeability of firn layers[177]; amplified melt owing to biological snow and ice darkening[229]; tidewater glacier acceleration and destabilization by submarine melting[34,230,231]; reduced buttressing effect from ice shelves[232]; accelerated interior motion from increased melt and rainfall[206]; enhanced basal thawing owing to hydraulically released latent heat and viscous warming[233]; and ice shelf flexure, (hydro)fracture and collapse in response to surface meltwater ponding and drainage[109,112,228]. The lack of representation of these processes in the modelling chain leads to deep uncertainty and could mean that future sea level rise projections are too conservative, motivating the high-end storyline in AR6 (ref. 3) or high-end mass loss estimates[234].

GCM and Earth system model projections typically underrepresent changes in atmospheric circulation and wind that are associated with increased Greenland atmospheric blocking[235,236] (Fig. 5). Reasons for the lack of consistency between models and observations have been suggested to stem from model biases in the forced response to anthropogenic emissions or in simulating tropical decadal variability[237]. Therefore, the projected surface melt increase of the GrIS could be misrepresented if the summer circulation changes that have been observed since the 1990s persist in the next decades[238]. Improved representation of Greenland atmospheric circulation and blocking changes in climate models is, therefore, a priority. A similar situation is seen for the AIS wherein models poorly represent surface air temperature and winds (Fig. 5).

Accurately simulating calving and damage processes using physics-based treatments is currently one of the greatest challenges in ice sheet modelling. The lack of a unified, physics-based treatment of calving processes contributes to the deep uncertainty in sea level projections for both ice sheets, especially the AIS[3,239]. By far, the highest sea level projections currently included in AR6 are produced by numerical simulations that contain a representation of MICI[1]. However, these projections are based on a simplified, untested and unverified implementation of MICI in a single ice sheet model[94], which requires two separate calving mechanisms: ice shelf collapse caused by hydrofracturing, followed by potential cliff failure[93,95]. At present, there is no scientific consensus about the physical basis and exact formulation of these mechanisms in simulations of large-scale ice sheet dynamics.

Attempts have been made to implement calving laws and damage mechanisms in ice sheet models[95,240,241]. However, ISMIP6 sea level projections do not consider AIS calving and damage in any ice sheet model[141], and ISMIP6 GrIS simulations only include a heavily parameterized representation of retreat caused by calving and submarine melting[63]. Therefore, there is an urgent need to improve the physical representation of ice sheet and ice shelf fracture, validate calving laws and implement robust algorithms for damage mechanics in numerical ice sheet models. However, such improvements must overcome the mismatch between the spatial scales of fracture and calving processes and the resolution of ice sheet scale models. Alongside investment in model development, the remotely sensed and in situ data sources outlined above offer an opportunity to validate such models.

Another challenge is achieving model representations of sub-shelf melting. Despite the development of sophisticated coupled ice–ocean models[136,242], which have greatly improved the ability to represent melt rates for complex time-evolving geometries and ocean properties, a number of challenges remain. To increase confidence in the representation of melt rates near the grounding line, wherein ice dynamics are particularly sensitive to basal melt, high-resolution numerical simulations constrained by satellite and in situ observations of past and present basal melt and seafloor bathymetry are required. Additionally, the two-way interaction between changes in ice shelf geometry (thinning, thickening and calving) and basal melt rates is key to simulating future mass loss from the AIS[140,243], yet these feedbacks remain poorly understood. For the GrIS, it is not yet possible to meaningfully couple ice sheet and ocean models across the many complex fjord systems, which are smaller than the resolution of regional ocean models; therefore, improved, higher-resolution models and better data are needed to bridge this gap. Obtaining improved observations of melt rates for changing cavity shapes and ocean conditions at annual to centennial timescales is, thus, a fundamental research priority.

Owing to the high computational cost of coupled ice–ocean simulations, most sea level projections are currently based on stand-alone ice sheet model simulations that use various simplified

melt parameterizations. Not only do spatial melt patterns vary greatly between these parameterizations, but AIS projections[131,141,244] have also revealed that the sensitivity of the parameterizations to changes in ocean temperature constitutes a major source of uncertainty. This limitation must be addressed by developing new calibration approaches based on transient ocean model simulations[245,246]. Co-ordinated ice sheet modelling exercises such as ISMIP6/7 are largely unfunded, community-driven efforts; therefore, to overcome the above-mentioned model limitations, it will be important that such co-ordinated modelling exercises receive appropriate funding.

Finally, another advancement that is becoming increasingly important in ice sheet modelling is the development and implementation of coupled ice sheet–Earth system models, such as UKESM and CESM2/3 (refs. 130,247,248), in which ice sheets can dynamically interact with the climate and wider Earth system. Ice sheet and coupled models can complement each other, and their harmony will be critical for achieving interconnected, global insight into the short-term and long-term variability of the Antarctic and Greenland ice sheets.

Published online: 08 February 2024

References

1. Hanna, E. et al. Mass balance of the ice sheets and glaciers — progress since AR5 and challenges. *Earth-Sci. Rev.* **201**, 102976 (2020).
2. Jia, Y., Xiao, K., Lin, M. & Zhang, X. Analysis of global sea level change based on multi-source data. *Remote Sens.* **14**, 4854 (2022).
3. Fox-Kemper, B., Hewitt, H. T. & Xiao, C. et al. in *IPCC: Climate Change 2021: The Physical Science Basis. Contribution of Working Group I to the Sixth 794 Assessment Report of the Intergovernmental Panel on Climate Change* (eds Masson-Delmotte, V. et al.) 1211–1361 (Cambridge Univ. Press, 2021).
4. Rack, W. & Rott, H. Pattern of retreat and disintegration of the Larsen B Ice Shelf, Antarctic Peninsula. *Ann. Glaciol.* **39**, 505–510 (2004).
5. Scambos, T. et al. Ice shelf disintegration by plate bending and hydro-fracture: satellite observations and model results of the 2008 Wilkins Ice Shelf break-ups. *Earth Planet. Sci. Lett.* **280**, 51–60 (2009).
6. Beckmann, J. & Winkelmann, R. Effects of extreme melt events on ice flow and sea level rise of the Greenland Ice Sheet. *Cryosphere* **17**, 3083–3099 (2023).
7. Grazioli, J. et al. Katabatic winds diminish precipitation contribution to the Antarctic ice mass balance. *Proc. Natl Acad. Sci. USA* **114**, 10858–10863 (2017).
8. Das, I. et al. Influence of persistent wind scour on the surface mass balance of Antarctica. *Nat. Geosci.* **6**, 367–371 (2013).
9. Medley, B., Lenaerts, J. T. M., Dattler, M., Keenan, E. & Wever, N. Predicting Antarctic net snow accumulation at the kilometer scale and its impact on observed height changes. *Geophys. Res. Lett.* **49**, e2022GL099330 (2022).
10. Maclennan, M. L., Lenaerts, J. T. M., Shields, C. & Wille, J. D. Contribution of atmospheric rivers to Antarctic precipitation. *Geophys. Res. Lett.* **49**, e2022GL100585 (2022).
11. Wille, J. D. et al. Antarctic atmospheric river climatology and precipitation impacts. *J. Geophys. Res. Atmos.* **126**, e2020JD033788 (2021).
12. Mattingly, K. S., Mote, T. L. & Fettweis, X. Atmospheric river impacts on Greenland Ice Sheet surface mass balance. *J. Geophys. Res. Atmos.* **123**, 8538–8560 (2018).
13. Turner, J. et al. The dominant role of extreme precipitation events in Antarctic snowfall variability. *Geophys. Res. Lett.* **46**, 3502–3511 (2019).
14. Box, J. E. et al. Greenland Ice Sheet rainfall, heat and albedo feedback impacts from the mid-August 2021 atmospheric river. *Geophys. Res. Lett.* **49**, e2021GL097356 (2022).
15. Lenaerts, J. T. M., Medley, B., van den Broeke, M. R. & Wouters, B. Observing and modeling ice sheet surface mass balance. *Rev. Geophys.* **57**, 376–420 (2019).
16. Ekaykin, A. A., Kozachek, A. V., Ya. Lipenkov, V. & Shibaev, Y. A. Multiple climate shifts in the Southern Hemisphere over the past three centuries based on central Antarctic snow pits and core studies. *Ann. Glaciol.* **55**, 259–266 (2014).
17. Ekaykin, A. A. et al. The changes in isotope composition and accumulation of snow at Vostok station, East Antarctica, over the past 200 years. *Ann. Glaciol.* **39**, 569–575 (2004).
18. Hanna, E., Cropper, T. E., Hall, R. J., Cornes, R. C. & Barriendos, M. Extended North Atlantic Oscillation and Greenland blocking indices 1800–2020 from new meteorological reanalysis. *Atmosphere* **13**, 436 (2022).
19. Hofer, S., Tedstone, A. J., Fettweis, X. & Bamber, J. L. Decreasing cloud cover drives the recent mass loss on the Greenland Ice Sheet. *Sci. Adv.* **3**, e1700584 (2017).
20. Noël, B., van de Berg, W. J., Lhermitte, S. & van den Broeke, M. R. Rapid ablation zone expansion amplifies north Greenland mass loss. *Sci. Adv.* **5**, eaaw0123 (2019).
21. Hermann, M., Papritz, L. & Wernli, H. Lagrangian analysis of the dynamical and thermodynamic drivers of Greenland melt events during 1979-2017. *Weather Clim. Dyn.* **1**, 497–518 (2020).
22. Shahi, S., Abermann, J., Heinrich, G., Prinz, R. & Schöner, W. Regional variability and trends of temperature inversions in Greenland. *J. Clim.* **33**, 9391–9407 (2020).
23. Tedesco, M. et al. The darkening of the Greenland Ice Sheet: trends, drivers, and projections (1981–2100). *Cryosphere* **10**, 477–496 (2016).
24. Van Tricht, K. et al. Clouds enhance Greenland Ice Sheet meltwater runoff. *Nat. Commun.* **7**, 10266 (2016).
25. Ding, Q. et al. Tropical forcing of the recent rapid Arctic warming in northeastern Canada and Greenland. *Nature* **509**, 209–212 (2014).
26. Hanna, E., Cropper, T. E., Hall, R. J. & Cappelen, J. Greenland Blocking Index 1851–2015: a regional climate change signal. *Int. J. Climatol.* **36**, 4847–4861 (2016).
27. Rignot, E. et al. Four decades of Antarctic Ice Sheet mass balance from 1979–2017. *Proc. Natl Acad. Sci.* **116**, 1095–1103 (2019).
28. Perren, B. B. et al. Southward migration of the Southern Hemisphere westerly winds corresponds with warming climate over centennial timescales. *Commun. Earth Environ.* **1**, 58 (2020).
29. Steig, E. J., Ding, Q., Battisti, D. S. & Jenkins, A. Tropical forcing of circumpolar deep water inflow and outlet glacier thinning in the Amundsen Sea Embayment, West Antarctica. *Ann. Glaciol.* **53**, 19–28 (2012).
30. Verfaillie, D. et al. The circum-Antarctic ice-shelves respond to a more positive Southern Annular Mode with regionally varied melting. *Commun. Earth Environ.* **3**, 139 (2022).
31. Medley, B. & Thomas, E. R. Increased snowfall over the Antarctic Ice Sheet mitigated twentieth-century sea-level rise. *Nat. Clim. Chang.* **9**, 34–39 (2019).
32. Munneke, P. K. et al. Elevation change of the Greenland Ice Sheet due to surface mass balance and firn processes, 1960–2014. *Cryosphere* **9**, 2009–2025 (2015).
33. van den Broeke, M. Depth and density of the Antarctic firn layer. *Arct. Antarct. Alp. Res.* **40**, 432–438 (2008).
34. Wood, M. et al. Ocean forcing drives glacier retreat in Greenland. *Sci. Adv.* **7**, eaba7282 (2021).
35. Jenkins, A. et al. West Antarctic Ice Sheet retreat in the Amundsen Sea driven by decadal oceanic variability. *Nat. Geosci.* **11**, 733–738 (2018).
36. Slater, D. A. & Straneo, F. Submarine melting of glaciers in Greenland amplified by atmospheric warming. *Nat. Geosci.* **15**, 794–799 (2022).
37. Straneo, F. & Heimbach, P. North Atlantic warming and the retreat of Greenland's outlet glaciers. *Nature* **504**, 36–43 (2013).
38. Fried, M. J. et al. Reconciling drivers of seasonal terminus advance and retreat at 13 Central West Greenland tidewater glaciers. *J. Geophys. Res.* **123**, 1590–1607 (2018).
39. O'Leary, M. & Christoffersen, P. Calving on tidewater glaciers amplified by submarine frontal melting. *Cryosphere* **7**, 119–128 (2013).
40. Catania, G. A., Stearns, L. A., Moon, T. A., Enderlin, E. M. & Jackson, R. H. Future evolution of Greenland's marine-terminating outlet glaciers. *J. Geophys. Res. Earth Surf.* **125**, e2018JF00487 (2020).
41. Bindschadler, R. et al. Getting around Antarctica: new high-resolution mappings of the grounded and freely-floating boundaries of the Antarctic Ice Sheet created for the International Polar Year. *Cryosphere* **5**, 569–588 (2011).
42. Smith, B. et al. Pervasive ice sheet mass loss reflects competing ocean and atmosphere processes. *Science* **368**, 1239–1242 (2020).
43. Pritchard, H. D. et al. Antarctic ice-sheet loss driven by basal melting of ice shelves. *Nature* **484**, 502–505 (2012).
44. Herraiz-Borreguero, L. & Naveira Garabato, A. C. Poleward shift of circumpolar deep water threatens the East Antarctic Ice Sheet. *Nat. Clim. Chang.* **12**, 728–734 (2022).
45. Greene, C. A., Gardner, A. S., Schlegel, N.-J. & Fraser, A. D. Antarctic calving loss rivals ice-shelf thinning. *Nature* **609**, 948–953 (2022).
46. Miles, B. W. J., Stokes, C. R. & Jamieson, S. S. R. Pan-ice-sheet glacier terminus change in East Antarctica reveals sensitivity of Wilkes Land to sea-ice changes. *Sci. Adv.* **2**, e1501350 (2016).
47. Greene, C. A., Blankenship, D. D., Gwyther, D. E., Silvano, A. & van Wijk, E. Wind causes Totten Ice Shelf melt and acceleration. *Sci. Adv.* **3**, e1701681 (2017).
48. Christie, F. D. W., Steig, E. J., Gourmelen, N., Tett, S. F. B. & Bingham, R. G. Inter-decadal climate variability induces differential ice response along Pacific-facing West Antarctica. *Nat. Commun.* **14**, 93 (2023).
49. Cook, A. J. et al. Ocean forcing of glacier retreat in the western Antarctic Peninsula. *Science* **353**, 283–286 (2016).
50. Naughten, K. A. et al. Simulated twentieth-century ocean warming in the Amundsen Sea, West Antarctica. *Geophys. Res. Lett.* **49**, e2021GL094566 (2022).
51. Nakayama, Y., Cai, C. & Seroussi, H. Impact of subglacial freshwater discharge on Pine Island Ice Shelf. *Geophys. Res. Lett.* **48**, e2021GL093923 (2021).
52. Dow, C. F., Ross, N., Jeofry, H., Siu, K. & Siegert, M. J. Antarctic basal environment shaped by high-pressure flow through a subglacial river system. *Nat. Geosci.* **15**, 892–898 (2022).
53. Christie, F. D. W. et al. Antarctic ice-shelf advance driven by anomalous atmospheric and sea-ice circulation. *Nat. Geosci.* **15**, 356–362 (2022).
54. Aoki, S. Breakup of land-fast sea ice in Lützow-Holm Bay, East Antarctica, and its teleconnection to tropical Pacific sea surface temperatures. *Geophys. Res. Lett.* **44**, 3219–3227 (2017).
55. Bromwich, D. H., Chen, B. & Hines, K. M. Global atmospheric impacts induced by year-round open water adjacent to Antarctica. *J. Geophys. Res. Atmos.* **103**, 11173–11189 (1998).
56. Wu, X., Budd, W. F., Lytle, V. I. & Massom, R. A. The effect of snow on Antarctic sea ice simulations in a coupled atmosphere-sea ice model. *Clim. Dyn.* **15**, 127–143 (1999).

57. Spolaor, A. et al. Halogen species record Antarctic sea ice extent over glacial–interglacial periods. *Atmos. Chem. Phys.* **13**, 6623–6635 (2013).
58. Landais, A. et al. Interglacial Antarctic–Southern Ocean climate decoupling due to moisture source area shifts. *Nat. Geosci.* **14**, 918–923 (2021).
59. Crosta, X. et al. Antarctic sea ice over the past 130,000 years, part 1: a review of what proxy records tell us. *Clim. Past* **18**, 1729–1756 (2022).
60. Massom, R. A. et al. Antarctic ice shelf disintegration triggered by sea ice loss and ocean swell. *Nature* **558**, 383–389 (2018).
61. Bell, R. E., Banwell, A. F., Trusel, L. D. & Kingslake, J. Antarctic surface hydrology and impacts on ice-sheet mass balance. *Nat. Clim. Chang.* **8**, 1044–1052 (2018).
62. Nienow, P. W., Sole, A. J., Slater, D. A. & Cowton, T. R. Recent advances in our understanding of the role of meltwater in the Greenland Ice Sheet system. *Curr. Clim. Change Rep.* **3**, 330–344 (2017).
63. Goelzer, H. et al. The future sea-level contribution of the Greenland Ice Sheet: a multi-model ensemble study of ISMIP6. *Cryosphere* **14**, 3071–3096 (2020).
64. Payne, A. J. et al. Future sea level change under Coupled Model Intercomparison Project Phase 5 and Phase 6 scenarios from the Greenland and Antarctic ice sheets. *Geophys. Res. Lett.* **48**, e2020GL091741 (2021).
65. Trusel, L. D. et al. Divergent trajectories of Antarctic surface melt under two twenty-first-century climate scenarios. *Nat. Geosci.* **8**, 927–932 (2015).
66. Jakobs, C. L., Reijmer, C. H., van den Broeke, M. R., van de Berg, W. J. & van Wessem, J. M. Spatial variability of the snowmelt-albedo feedback in Antarctica. *J. Geophys. Res. Earth Surf.* **126**, e2020JF005696 (2021).
67. Arthur, J. F., Stokes, C., Jamieson, S. S. R., Rachel Carr, J. & Leeson, A. A. Recent understanding of Antarctic supraglacial lakes using satellite remote sensing. *Prog. Phys. Geogr. Earth Environ.* **44**, 837–869 (2020).
68. IMBIE Team Mass balance of the Greenland Ice Sheet from 1992 to 2018. *Nature* **579**, 233–239 (2020).
69. Banwell, A. F., Wever, N., Dunmire, D. & Picard, G. Quantifying Antarctic-wide ice-shelf surface melt volume using microwave and firn model data: 1980 to 2021. *Geophys. Res. Lett.* **50**, e2023GL102744 (2023).
70. Banwell, A. F. & Macayeal, D. R. Ice-shelf fracture due to viscoelastic flexure stress induced by fill/drain cycles of supraglacial lakes. *Antarct. Sci.* **27**, 587–597 (2015).
71. Lai, C.-Y. et al. Vulnerability of Antarctica's ice shelves to meltwater-driven fracture. *Nature* **584**, 574–578 (2020).
72. van Wessem, J. M., van den Broeke, M. R., Wouters, B. & Lhermitte, S. Variable temperature thresholds of melt pond formation on Antarctic ice shelves. *Nat. Clim. Chang.* **13**, 161–166 (2023).
73. Alley, K. E., Scambos, T. A., Miller, J. Z., Long, D. G. & MacFerrin, M. Quantifying vulnerability of Antarctic ice shelves to hydrofracture using microwave scattering properties. *Remote Sens. Environ.* **210**, 297–306 (2018).
74. Scambos, T. A. Glacier acceleration and thinning after ice shelf collapse in the Larsen B Embayment, Antarctica. *Geophys. Res. Lett.* **31**, L18402 (2004).
75. Williams, J. J., Gourmelen, N. & Nienow, P. Dynamic response of the Greenland Ice Sheet to recent cooling. *Sci. Rep.* **10**, 1647 (2020).
76. Tuckett, P. A. et al. Rapid accelerations of Antarctic Peninsula outlet glaciers driven by surface melt. *Nat. Commun.* **10**, 4311 (2019).
77. Boxall, K., Christie, F. D. W., Willis, I. C., Wuite, J. & Nagler, T. Seasonal land-ice-flow variability in the Antarctic Peninsula. *Cryosphere* **16**, 3907–3932 (2022).
78. Payne, T., Nowicki, S., Goelzer, H. and the ISMIP6 Team. Contrasting contributions to future sea level under CMIP5 and CMIP6 scenarios from the Greenland and Antarctic ice sheets. https://doi.org/10.5194/egusphere-egu2020-11667 (2020).
79. Jamieson, S. S. R. et al. Ice-stream stability on a reverse bed slope. *Nat. Geosci.* **5**, 799–802 (2012).
80. Bart, P. J., DeCesare, M., Rosenheim, B. E., Majewski, W. & McGlannan, A. A centuries-long delay between a paleo-ice-shelf collapse and grounding-line retreat in the Whales Deep Basin, eastern Ross Sea, Antarctica. *Sci. Rep.* **8**, 12392 (2018).
81. Dowdeswell, J. A. et al. Delicate seafloor landforms reveal past Antarctic grounding-line retreat of kilometers per year. *Science* **368**, 1020–1024 (2020).
82. Graham, A. G. C. et al. Rapid retreat of Thwaites Glacier in the pre-satellite era. *Nat. Geosci.* **15**, 706–713 (2022).
83. Barletta, V. R. et al. Observed rapid bedrock uplift in Amundsen Sea Embayment promotes ice-sheet stability. *Science* **360**, 1335–1339 (2018).
84. Whitehouse, P. L. Glacial isostatic adjustment modelling: historical perspectives, recent advances, and future directions. *Earth Surf. Dyn.* **6**, 401–429 (2018).
85. Milillo, P. et al. Heterogeneous retreat and ice melt of Thwaites Glacier, West Antarctica. *Sci. Adv.* **5**, eaau3433 (2019).
86. Park, J. W. et al. Sustained retreat of the Pine Island Glacier. *Geophys. Res. Lett.* **40**, 2137–2142 (2013).
87. Hill, E. A. et al. The stability of present-day Antarctic grounding lines — part 1: no indication of marine ice sheet instability in the current geometry. *Cryosphere* **17**, 3739–3759 (2023).
88. Reese, R. et al. The stability of present-day Antarctic grounding lines — part 2: onset of irreversible retreat of Amundsen Sea glaciers under current climate on centennial timescales cannot be excluded. *Cryosphere* **17**, 3761–3783 (2023).
89. Rignot, E., Mouginot, J., Morlighem, M., Seroussi, H. & Scheuchl, B. Widespread, rapid grounding line retreat of Pine Island, Thwaites, Smith, and Kohler glaciers, West Antarctica, from 1992 to 2011. *Geophys. Res. Lett.* **41**, 3502–3509 (2014).
90. Joughin, I., Smith, B. E. & Medley, B. Marine ice sheet collapse potentially under way for the Thwaites Glacier Basin, West Antarctica. *Science* **344**, 735–738 (2014).
91. Schoof, C. Ice sheet grounding line dynamics: steady states, stability, and hysteresis. *J. Geophys. Res. Earth Surf.* **112**, F03S28 (2007).
92. DeConto, R. M. et al. The Paris Climate Agreement and future sea-level rise from Antarctica. *Nature* **593**, 83–89 (2021).
93. Pollard, D., DeConto, R. M. & Alley, R. B. Potential Antarctic Ice Sheet retreat driven by hydrofracturing and ice cliff failure. *Earth Planet. Sci. Lett.* **412**, 112–121 (2015).
94. DeConto, R. M. & Pollard, D. Contribution of Antarctica to past and future sea-level rise. *Nature* **531**, 591–597 (2016).
95. Crawford, A. J. et al. Marine ice-cliff instability modeling shows mixed-mode ice-cliff failure and yields calving rate parameterization. *Nat. Commun.* **12**, 2701 (2021).
96. Padman, L., Howard, S. L., Orsi, A. H. & Muench, R. D. Tides of the northwestern Ross Sea and their impact on dense outflows of Antarctic Bottom Water. *Deep Sea Res. Part II Top. Stud. Oceanogr.* **56**, 818–834 (2009).
97. Stewart, A. L., Klocker, A. & Menemenlis, D. Circum-Antarctic shoreward heat transport derived from an eddy- and tide-resolving simulation. *Geophys. Res. Lett.* **45**, 834–845 (2018).
98. Padman, L., Siegfried, M. R. & Fricker, H. A. Ocean tide influences on the Antarctic and Greenland ice sheets. *Rev. Geophys.* **56**, 142–184 (2018).
99. Richter, O., Gwyther, D. E., King, M. A. & Galton-Fenzi, B. K. The impact of tides on Antarctic ice shelf melting. *Cryosphere* **16**, 1409–1429 (2022).
100. Chen, H., Rignot, E., Scheuchl, B. & Ehrenfeucht, S. Grounding zone of Amery ice shelf, Antarctica, from differential synthetic-aperture radar interferometry. *Geophys. Res. Lett.* **50**, e2022GL102430 (2023).
101. Ciracì, E. et al. Melt rates in the kilometer-size grounding zone of Petermann Glacier, Greenland, before and during a retreat. *Proc. Natl Acad. Sci. USA* **120**, e2220924120 (2023).
102. Davison, B. J. et al. Sea level rise from West Antarctic mass loss significantly modified by large snowfall anomalies. *Nat. Commun.* **14**, 1479 (2023).
103. Adusumilli, S., Fricker, H. A., Medley, B., Padman, L. & Siegfried, M. R. Interannual variations in meltwater input to the Southern Ocean from Antarctic ice shelves. *Nat. Geosci.* **13**, 616–620 (2020).
104. Jenkins, A. et al. Decadal ocean forcing and Antarctic Ice Sheet response: lessons from the Amundsen Sea. *Oceanography* **29**, 106–117 (2016).
105. Paolo, F. S. et al. Response of Pacific-sector Antarctic ice shelves to the El Niño/Southern Oscillation. *Nat. Geosci.* **11**, 121–126 (2018).
106. Gwyther, D. E., O'Kane, T. J., Galton-Fenzi, B. K., Monselesan, D. P. & Greenbaum, J. S. Intrinsic processes drive variability in basal melting of the Totten Glacier ice shelf. *Nat. Commun.* **9**, 3141 (2018).
107. Hattermann, T. et al. Observed interannual changes beneath Filchner-Ronne Ice Shelf linked to large-scale atmospheric circulation. *Nat. Commun.* **12**, 2961 (2021).
108. Domack, E. et al. Stability of the Larsen B Ice Shelf on the Antarctic Peninsula during the Holocene epoch. *Nature* **436**, 681–685 (2005).
109. Leeson, A. A., Forster, E., Rice, A., Gourmelen, N. & Wessem, J. M. Evolution of supraglacial lakes on the Larsen B Ice Shelf in the decades before it collapsed. *Geophys. Res. Lett.* **47**, e2019 GL085591 (2020).
110. Banwell, A. F., MacAyeal, D. R. & Sergienko, O. V. Breakup of the Larsen B Ice Shelf triggered by chain reaction drainage of supraglacial lakes. *Geophys. Res. Lett.* **40**, 5872–5876 (2013).
111. Scambos, T. A., Hulbe, C., Fahnestock, M. & Bohlander, J. The link between climate warming and break-up of ice shelves in the Antarctic Peninsula. *J. Glaciol.* **46**, 516–530 (2000).
112. Robel, A. A. & Banwell, A. F. A speed limit on ice shelf collapse through hydrofracture. *Geophys. Res. Lett.* **46**, 12092–12100 (2019).
113. Pritchard, H. D. & Vaughan, D. G. Widespread acceleration of tidewater glaciers on the Antarctic Peninsula. *J. Geophys. Res.* **112**, F03S29 (2007).
114. Wille, J. D. et al. Intense atmospheric rivers can weaken ice shelf stability at the Antarctic Peninsula. *Commun. Earth Environ.* **3**, 90 (2022).
115. Bozkurt, D., Rondanelli, R., Marín, J. C. & Garreaud, R. Foehn event triggered by an atmospheric river underlies record-setting temperature along continental Antarctica. *J. Geophys. Res.* **123**, 3871–3892 (2018).
116. Hodgson, D. A., Jordan, T. A., Ross, N., Riley, T. R. & Fretwell, P. T. Drainage and refill of an Antarctic Peninsula subglacial lake reveal an active subglacial hydrological network. *Cryosphere* **16**, 4797–4809 (2022).
117. Bintanja, R., van de Wal, R. S. W. & Oerlemans, J. Modelled atmospheric temperatures and global sea levels over the past million years. *Nature* **437**, 125–128 (2005).
118. Bronselaer, B. et al. Change in future climate due to Antarctic meltwater. *Nature* **564**, 53–58 (2018).
119. Sadai, S., Condron, A., DeConto, R. & Pollard, D. Future climate response to Antarctic Ice Sheet melt caused by anthropogenic warming. *Sci. Adv.* **6**, eaaz1169 (2020).
120. Silvano, A. et al. Freshening by glacial meltwater enhances melting of ice shelves and reduces formation of Antarctic Bottom Water. *Sci. Adv.* **4**, eaap9467 (2018).
121. Dutton, A. et al. Sea-level rise due to polar ice-sheet mass loss during past warm periods. *Science* **349**, aaa4019 (2015).
122. Dumitru, O. A. et al. Constraints on global mean sea level during Pliocene warmth. *Nature* **574**, 233–236 (2019).
123. Sangiorgi, F. et al. Southern Ocean warming and Wilkes Land ice sheet retreat during the mid-Miocene. *Nat. Commun.* **9**, 317 (2018).
124. Naish, T. et al. Obliquity-paced Pliocene West Antarctic Ice Sheet oscillations. *Nature* **458**, 322–328 (2009).

125. Cook, C. P. et al. Dynamic behaviour of the East Antarctic Ice Sheet during Pliocene warmth. *Nat. Geosci.* **6**, 765–769 (2013).
126. Wilson, D. J. et al. Ice loss from the East Antarctic Ice Sheet during late Pleistocene interglacials. *Nature* **561**, 383–386 (2018).
127. Crotti, I. et al. Wilkes subglacial basin ice sheet response to Southern Ocean warming during late Pleistocene interglacials. *Nat. Commun.* **13**, 5328 (2022).
128. Blackburn, T. et al. Ice retreat in Wilkes Basin of East Antarctica during a warm interglacial. *Nature* **583**, 554–559 (2020).
129. Tewari, K., Mishra, S. K., Salunke, P. & Dewan, A. Future projections of temperature and precipitation for Antarctica. *Environ. Res. Lett.* **17**, 014029 (2022).
130. Dunmire, D., Lenaerts, J. T. M., Datta, R. T. & Gorte, T. Antarctic surface climate and surface mass balance in the Community Earth System Model version 2 during the satellite era and into the future (1979–2100). *Cryosphere* **16**, 4163–4184 (2022).
131. Edwards, T. L. et al. Projected land ice contributions to twenty-first-century sea level rise. *Nature* **593**, 74–82 (2021).
132. Jourdain, N. C., Mathiot, P., Burgard, C., Caillet, J. & Kittel, C. Ice shelf basal melt rates in the Amundsen Sea at the end of the 21st century. *Geophys. Res. Lett.* **49**, e2022GL100629 (2022).
133. Golledge, N. R. et al. Global environmental consequences of twenty-first-century ice-sheet melt. *Nature* **566**, 65–72 (2019).
134. Hellmer, H. H., Kauker, F., Timmermann, R., Determann, J. & Rae, J. Twenty-first-century warming of a large Antarctic ice-shelf cavity by a redirected coastal current. *Nature* **485**, 225–228 (2012).
135. Hellmer, H. H., Kauker, F., Timmermann, R. & Hattermann, T. The fate of the southern Weddell Sea continental shelf in a warming climate. *J. Clim.* **30**, 4337–4350 (2017).
136. Naughten, K. A. et al. Two-timescale response of a large Antarctic Ice Shelf to climate change. *Nat. Commun.* **12**, 1991 (2021).
137. Christianson, K. et al. Sensitivity of Pine Island Glacier to observed ocean forcing. *Geophys. Res. Lett.* **43**, 10817–10825 (2016).
138. Milillo, P. et al. Rapid glacier retreat rates observed in West Antarctica. *Nat. Geosci.* **15**, 48–53 (2022).
139. Goldberg, D. N. et al. Representing grounding line migration in synchronous coupling between a marine ice sheet model and a z-coordinate ocean model. *Ocean Model.* **125**, 45–60 (2018).
140. De Rydt, J., De Rydt, J. & Gudmundsson, G. H. Coupled ice shelf-ocean modeling and complex grounding line retreat from a seabed ridge. *J. Geophys. Res. Earth Surf.* **121**, 865–880 (2016).
141. Seroussi, H. et al. ISMIP6 Antarctica: a multi-model ensemble of the Antarctic Ice Sheet evolution over the 21st century. *Cryosphere* **14**, 3033–3070 (2020).
142. Dutrieux, P. et al. Strong sensitivity of Pine Island ice-shelf melting to climatic variability. *Science* **343**, 174–178 (2014).
143. Smith, J. A. et al. Sub-ice-shelf sediments record history of twentieth-century retreat of Pine Island Glacier. *Nature* **541**, 77–80 (2017).
144. Holland, P. R., Bracegirdle, T. J., Dutrieux, P., Jenkins, A. & Steig, E. J. West Antarctic ice loss influenced by internal climate variability and anthropogenic forcing. *Nat. Geosci.* **12**, 718–724 (2019).
145. Holland, P. R. et al. Anthropogenic and internal drivers of wind changes over the Amundsen Sea, West Antarctica, during the 20th and 21st centuries. *Cryosphere* **16**, 5085–5105 (2022).
146. Batchelor, C. L. et al. Rapid, buoyancy-driven ice-sheet retreat of hundreds of metres per day. *Nature* **617**, 105–110 (2023).
147. Tedesco, M. & Fettweis, X. Unprecedented atmospheric conditions (1948–2019) drive the 2019 exceptional melting season over the Greenland Ice Sheet. *Cryosphere* **14**, 1209–1223 (2020).
148. Otosaka, I. N. et al. Mass balance of the Greenland and Antarctic ice sheets from 1992 to 2020. *Earth Syst. Sci. Data* **15**, 1597–1616 (2023).
149. Moon, T. A. et al. NOAA Arctic Report Card 2022: Greenland Ice Sheet. https://doi.org/10.25923/C430-HB50 (2022).
150. Bartholomew, I. D. et al. Seasonal variations in Greenland Ice Sheet motion: inland extent and behaviour at higher elevations. *Earth Planet. Sci. Lett.* **307**, 271–278 (2011).
151. Rathmann, N. M. et al. Highly temporally resolved response to seasonal surface melt of the Zachariae and 79N outlet glaciers in northeast Greenland. *Geophys. Res. Lett.* **44**, 9805–9814 (2017).
152. Larsen, S. H. et al. Outlet glacier flow response to surface melt: based on analysis of a high-resolution satellite data set. *J. Glaciol.* **69**, 1047–1055 (2023).
153. Moon, T. et al. Distinct patterns of seasonal Greenland glacier velocity. *Geophys. Res. Lett.* **41**, 7209–7216 (2014).
154. Stevens, L. A. et al. Tidewater-glacier response to supraglacial lake drainage. *Nat. Commun.* **13**, 6065 (2022).
155. Solgaard, A. M., Noël, D. R. & Hviberg, C. S. Seasonal patterns of Greenland ice velocity from Sentinel-1 SAR data linked to runoff. *Geophys. Res. Lett.* **49**, e2022GL100343 (2022).
156. Mattingly, K. S., Ramseyer, C. A., Rosen, J. J., Mote, T. L. & Muthyala, R. Increasing water vapor transport to the Greenland Ice Sheet revealed using self-organizing maps: increasing Greenland moisture transport. *Geophys. Res. Lett.* **43**, 9250–9258 (2016).
157. Hanna, E. et al. Greenland surface air temperature changes from 1981 to 2019 and implications for ice-sheet melt and mass-balance change. *Int. J. Climatol.* **41**, E1336–E1352 (2021).
158. Niwano, M. et al. Rainfall on the Greenland Ice Sheet: present-day climatology from a high-resolution non-hydrostatic polar regional climate model. *Geophys. Res. Lett.* **48**, e2021GL092942 (2021).
159. Nettles, M. et al. Step-wise changes in glacier flow speed coincide with calving and glacial earthquakes at Helheim Glacier, Greenland. *Geophys. Res. Lett.* **35**, L24503 (2008).
160. Cassotto, R. et al. Non-linear glacier response to calving events, Jakobshavn Isbræ, Greenland. *J. Glaciol.* **65**, 39–54 (2019).
161. Amundson, J. M., Truffer, M. & Zwinger, T. Tidewater glacier response to individual calving events. *J. Glaciol.* **68**, 1117–1126 (2022).
162. Khan, S. A., Wahr, J., Bevis, M., Velicogna, I. & Kendrick, E. Spread of ice mass loss into Northwest Greenland observed by GRACE and GPS. *Geophys. Res. Lett.* **37**, L06501 (2010).
163. Chauché, N., Hubbard, A., Gascard, J. C. & Box, J. E. Ice–ocean interaction and calving front morphology at two west Greenland tidewater outlet glaciers. *Cryosphere* **8**, 1457–1468 (2014).
164. Cook, S. et al. Modelling environmental influences on calving at Helheim Glacier in eastern Greenland. *Cryosphere* **8**, 827–841 (2014).
165. Catania, G. A. et al. Geometric controls on tidewater glacier retreat in central western Greenland. *J. Geophys. Res. Earth Surf.* **123**, 2024–2038 (2018).
166. Enderlin, E. M., Howat, I. M. & Vieli, A. High sensitivity of tidewater outlet glacier dynamics to shape. *Cryosphere* **7**, 1007–1015 (2013).
167. de Juan, J. et al. Sudden increase in tidal response linked to calving and acceleration at a large Greenland outlet glacier. *Geophys. Res. Lett.* **37**, L12501 (2010).
168. van Dongen, E. et al. Tides modulate crevasse opening prior to a major calving event at Bowdoin Glacier, Northwest Greenland. *J. Glaciol.* **66**, 113–123 (2020).
169. Ma, Y. & Bassis, J. N. The effect of submarine melting on calving from marine terminating glaciers. *J. Geophys. Res.* **124**, 334–346 (2019).
170. van Dongen, E. C. H. et al. Numerical modeling shows increased fracturing due to melt-undercutting prior to major calving at Bowdoin Glacier. *Front. Earth Sci.* **8**, 253 (2020).
171. Cassotto, R., Fahnestock, M., Amundson, J. M., Truffer, M. & Joughin, I. Seasonal and interannual variations in ice melange and its impact on terminus stability, Jakobshavn Isbræ, Greenland. *J. Glaciol.* **61**, 76–88 (2015).
172. Moon, T., Joughin, I. & Smith, B. Seasonal to multiyear variability of glacier surface velocity, terminus position, and sea ice/ice mélange in Northwest Greenland. *J. Geophys. Res.* **120**, 818–833 (2015).
173. Box, J. E. et al. Greenland Ice Sheet climate disequilibrium and committed sea-level rise. *Nat. Clim. Chang.* **12**, 808–813 (2022).
174. Fettweis, X. et al. GrSMBMIP: intercomparison of the modelled 1980–2012 surface mass balance over the Greenland Ice Sheet. *Cryosphere* **14**, 3935–3958 (2020).
175. Trusel, L. D. et al. Nonlinear rise in Greenland runoff in response to post-industrial Arctic warming. *Nature* **564**, 104–108 (2018).
176. Box, J. E. et al. Greenland Ice Sheet mass balance reconstruction. Part I: net snow accumulation (1600–2009). *J. Clim.* **26**, 3919–3934 (2013).
177. MacFerrin, M. et al. Rapid expansion of Greenland's low-permeability ice slabs. *Nature* **573**, 403–407 (2019).
178. Culberg, R., Schroeder, D. M. & Chu, W. Extreme melt season ice layers reduce firn permeability across Greenland. *Nat. Commun.* **12**, 2336 (2021).
179. Tedstone, A. J. & Machguth, H. Increasing surface runoff from Greenland's firn areas. *Nat. Clim. Chang.* **12**, 672–676 (2022).
180. Ryan, J. C. et al. Greenland Ice Sheet surface melt amplified by snowline migration and bare ice exposure. *Sci. Adv.* **5**, eaav3738 (2019).
181. Horlings, A. N., Christianson, K. & Miège, C. Expansion of firn aquifers in Southeast Greenland. *J. Geophys. Res.* **127**, e2022JF006753 (2022).
182. NEEM community members. Eemian interglacial reconstructed from a Greenland folded ice core. *Nature* **493**, 489–494 (2013).
183. Vinther, B. M. et al. Holocene thinning of the Greenland Ice Sheet. *Nature* **461**, 385–388 (2009).
184. Sasgen, I. et al. Return to rapid ice loss in Greenland and record loss in 2019 detected by the GRACE-FO satellites. *Commun. Earth Environ.* **1**, 8 (2020).
185. Mankoff, K. D. et al. Greenland Ice Sheet mass balance from 1840 through next week. *Earth Syst. Sci. Data* **13**, 5001–5025 (2021).
186. Fettweis, X. et al. Reconstructions of the 1900–2015 Greenland Ice Sheet surface mass balance using the regional climate MAR model. *Cryosphere* **11**, 1015–1033 (2017).
187. Noël, B., Lenaerts, J. T. M., Lipscomb, W. H., Thayer-Calder, K. & van den Broeke, M. R. Peak refreezing in the Greenland firn layer under future warming scenarios. *Nat. Commun.* **13**, 6870 (2022).
188. Noël, B., van Kampenhout, L., Lenaerts, J. T. M., van de Berg, W. J. & van den Broeke, M. R. A 21st century warming threshold for sustained Greenland Ice Sheet mass loss. *Geophys. Res. Lett.* **48**, e2020GL090471 (2021).
189. clec'h, S. L. et al. Assessment of the Greenland Ice Sheet–atmosphere feedbacks for the next century with a regional atmospheric model coupled to an ice sheet model. *Cryosphere* **13**, 373–395 (2019).
190. Boberg, F., Mottram, R., Hansen, N., Yang, S. & Langen, P. L. Uncertainties in projected surface mass balance over the polar ice sheets from dynamically downscaled EC-Earth models. *Cryosphere* **16**, 17–33 (2022).
191. Robinson, A., Calov, R. & Ganopolski, A. Multistability and critical thresholds of the Greenland Ice Sheet. *Nat. Clim. Chang.* **2**, 429–432 (2012).

192. Aschwanden, A. et al. Contribution of the Greenland Ice Sheet to sea level over the next millennium. *Sci. Adv.* **5**, eaav9396 (2019).
193. Gregory, J. M., George, S. E. & Smith, R. S. Large and irreversible future decline of the Greenland Ice Sheet. *Cryosphere* **14**, 4299–4322 (2020).
194. Ultee, L., Felikson, D., Minchew, B., Stearns, L. A. & Riel, B. Helheim Glacier ice velocity variability responds to runoff and terminus position change at different timescales. *Nat. Commun.* **13**, 6022 (2022).
195. Holland, D. M., Thomas, R. H., de Young, B., Ribergaard, M. H. & Lyberth, B. Acceleration of Jakobshavn Isbræ triggered by warm subsurface ocean waters. *Nat. Geosci.* **1**, 659–664 (2008).
196. Barnett, J., Holmes, F. A. & Kirchner, N. Modelled dynamic retreat of Kangerlussuaq Glacier, East Greenland, strongly influenced by the consecutive absence of an ice mélange in Kangerlussuaq Fjord. *J. Glaciol.* **69**, 433–444 (2022).
197. Christian, J. E. et al. The contrasting response of outlet glaciers to interior and ocean forcing. *Cryosphere* **14**, 2515–2535 (2020).
198. Grinsted, A. et al. Accelerating ice flow at the onset of the Northeast Greenland ice stream. *Nat. Commun.* **13**, 5589 (2022).
199. Zwally, H. J. et al. Surface melt-induced acceleration of Greenland ice-sheet flow. *Science* **297**, 218–222 (2002).
200. Wal et al. Self-regulation of ice flow varies across the ablation area in south-west Greenland. *Cryosphere* **9**, 603–611 (2015).
201. Tedstone, A. J. et al. Decadal slowdown of a land-terminating sector of the Greenland Ice Sheet despite warming. *Nature* **526**, 692–695 (2015).
202. Sole, A. et al. Winter motion mediates dynamic response of the Greenland Ice Sheet to warmer summers. *Geophys. Res. Lett.* **40**, 3940–3944 (2013).
203. Andersen, M. L. et al. Quantitative estimates of velocity sensitivity to surface melt variations at a large Greenland outlet glacier. *J. Glaciol.* **57**, 609–620 (2011).
204. Doyle, S. H. et al. Persistent flow acceleration within the interior of the Greenland Ice Sheet. *Geophys. Res. Lett.* **41**, 899–905 (2014).
205. Clason, C. C. et al. Modelling the transfer of supraglacial meltwater to the bed of Leverett Glacier, Southwest Greenland. *Cryosphere* **9**, 123–138 (2015).
206. Doyle, S. H. et al. Amplified melt and flow of the Greenland Ice Sheet driven by late-summer cyclonic rainfall. *Nat. Geosci.* **8**, 647–653 (2015).
207. Rignot, E. & Kanagaratnam, P. Changes in the velocity structure of the Greenland Ice Sheet. *Science* **311**, 986–990 (2006).
208. Bassis, J. N. The statistical physics of iceberg calving and the emergence of universal calving laws. *J. Glaciol.* **57**, 3–16 (2011).
209. Luckman, A., Murray, T., de Lange, R. & Hanna, E. Rapid and synchronous ice-dynamic changes in East Greenland. *Geophys. Res. Lett.* **33**, L03503 (2006).
210. Csatho, B., Schenk, T., Van Der Veen, C. J. & Krabill, W. B. Intermittent thinning of Jakobshavn Isbræ, West Greenland, since the little ice age. *J. Glaciol.* **54**, 131–144 (2008).
211. Nick, F. M., Vieli, A., Howat, I. M. & Joughin, I. Large-scale changes in Greenland outlet glacier dynamics triggered at the terminus. *Nat. Geosci.* **2**, 110–114 (2009).
212. Felikson, D. et al. Inland thinning on the Greenland Ice Sheet controlled by outlet glacier geometry. *Nat. Geosci.* **10**, 366–369 (2017).
213. Khan, S. A. et al. Extensive inland thinning and speed-up of Northeast Greenland Ice Stream. *Nature* **611**, 727–732 (2022).
214. Kehrl, L. M., Joughin, I., Shean, D. E., Floricioiu, D. & Krieger, L. Seasonal and interannual variabilities in terminus position, glacier velocity, and surface elevation at Helheim and Kangerlussuaq glaciers from 2008 to 2016. *J. Geophys. Res.* **122**, 1635–1652 (2017).
215. Robel, A. A., Seroussi, H. & Roe, G. H. Marine ice sheet instability amplifies and skews uncertainty in projections of future sea-level rise. *Proc. Natl Acad. Sci. USA* **116**, 14887–14892 (2019).
216. Felikson, D., Nowicki, S., Nias, I., Morlighem, M. & Seroussi, H. Seasonal tidewater glacier terminus oscillations bias multi-decadal projections of ice mass change. *J. Geophys. Res.* **127**, e2021JF006249 (2022).
217. Tapley, B. D. et al. Contributions of GRACE to understanding climate change. *Nat. Clim. Chang.* **5**, 358–369 (2019).
218. Rees, E. R. et al. Absolute frequency readout derived from ULE cavity for next generation geodesy missions. *Opt. Express* **29**, 26014–26027 (2021).
219. Flechtner, F. et al. What can be expected from the GRACE-FO laser ranging interferometer for Earth science applications? *Surv. Geophys.* **37**, 453–470 (2016).
220. ESA Earth and Mission Science Division & NASA Earth Science Division. *Next Generation Gravity Mission as a Mass-change And Geosciences International Constellation (MAGIC) Mission Requirements Document* (eds Haagmans, R. & Tsaoussi, L.) (ESA and NASA, 2020).
221. Davis, P. E. D. et al. Suppressed basal melting in the eastern Thwaites Glacier grounding zone. *Nature* **614**, 479–485 (2023).
222. Schmidt, B. E. et al. Heterogeneous melting near the Thwaites Glacier grounding line. *Nature* **614**, 471–478 (2023).
223. Vaňková, I. & Nicholls, K. W. Ocean variability beneath the Filchner-Ronne ice shelf inferred from basal melt rate time series. *J. Geophys. Res. Ocean.* **127**, e2022JC018879 (2022).
224. Sutherland, D. A. et al. Direct observations of submarine melt and subsurface geometry at a tidewater glacier. *Science* **365**, 369–374 (2019).
225. Morlighem, M. et al. Deep glacial troughs and stabilizing ridges unveiled beneath the margins of the Antarctic Ice Sheet. *Nat. Geosci.* **13**, 132–137 (2020).
226. Colleoni, F. et al. Spatio-temporal variability of processes across Antarctic ice-bed-ocean interfaces. *Nat. Commun.* **9**, 2289 (2018).
227. Zheng, L. et al. Greenland Ice Sheet daily surface melt flux observed from space. *Geophys. Res. Lett.* **49**, e2021GL096690 (2022).
228. Banwell, A. F., Willis, I. C., Macdonald, G. J., Goodsell, B. & MacAyeal, D. R. Direct measurements of ice-shelf flexure caused by surface meltwater ponding and drainage. *Nat. Commun.* **10**, 730 (2019).
229. Stibal, M. et al. Algae drive enhanced darkening of bare ice on the Greenland Ice Sheet. *Geophys. Res. Lett.* **44**, 11,463–11,471 (2017).
230. Khazendar, A. et al. Author correction: Interruption of two decades of Jakobshavn Isbrae acceleration and thinning as regional ocean cools. *Nat. Geosci.* **12**, 493–493 (2019).
231. Truffer, M. & Fahnestock, M. Climate change: rethinking ice sheet time scales. *Science* **315**, 1508–1510 (2007).
232. Mouginot, J. et al. Fast retreat of Zachariæ Isstrøm, Northeast Greenland. *Science* **350**, 1357–1361 (2015).
233. Phillips, T., Rajaram, H. & Steffen, K. Cryo-hydrologic warming: a potential mechanism for rapid thermal response of ice sheets. *Geophys. Res. Lett.* **37**, L20503 (2010).
234. van de Wal, R. S. W. et al. A high-end estimate of sea level rise for practitioners. *Earths Future* **10**, e2022EF002751 (2022).
235. Fettweis, X. et al. *Brief communication* 'Important role of the mid-tropospheric atmospheric circulation in the recent surface melt increase over the Greenland Ice Sheet'. *Cryosphere* **7**, 241–248 (2013).
236. Topál, D. et al. Discrepancies between observations and climate models of large-scale wind-driven Greenland melt influence sea-level rise projections. *Nat. Commun.* **13**, 6833 (2022).
237. Topál, D. & Ding, Q. Atmospheric circulation-constrained model sensitivity recalibrates Arctic climate projections. *Nat. Clim. Chang.* **13**, 710–718 (2023).
238. Delhasse, A., Fettweis, X., Kittel, C., Amory, C. & Agosta, C. Brief communication: Impact of the recent atmospheric circulation change in summer on the future surface mass balance of the Greenland Ice Sheet. *Cryosphere* **12**, 3409–3418 (2018).
239. Benn, D. I., Cowton, T., Todd, J. & Luckman, A. Glacier calving in Greenland. *Curr. Clim. Chang. Rep.* **3**, 282–290 (2017).
240. Sun, S., Cornford, S. L., Moore, J. C., Gladstone, R. & Zhao, L. Ice shelf fracture parameterization in an ice sheet model. *Cryosphere* **11**, 2543–2554 (2017).
241. Krug, J., Weiss, J., Gagliardini, O. & Durand, G. Combining damage and fracture mechanics to model calving. *Cryosphere* **8**, 2101–2117 (2014).
242. Smith, R. S. et al. Coupling the U.K. Earth System Model to dynamic models of the Greenland and Antarctic ice sheets. *J. Adv. Model. Earth Syst.* **13**, e2021MS002520 (2021).
243. Bradley, A. T., Bett, D. T., Dutrieux, P., De Rydt, J. & Holland, P. R. The influence of Pine Island ice shelf calving on basal melting. *J. Geophys. Res. Ocean.* **127**, e2022JC018621 (2022).
244. Reese, R., Levermann, A., Albrecht, T., Seroussi, H. & Winkelmann, R. The role of history and strength of the oceanic forcing in sea level projections from Antarctica with the Parallel Ice Sheet Model. *Cryosphere* **14**, 3097–3110 (2020).
245. Jourdain, N. C. et al. A protocol for calculating basal melt rates in the ISMIP6 Antarctic Ice Sheet projections. *Cryosphere* **14**, 3111–3134 (2020).
246. Burgard, C., Jourdain, N. C., Reese, R., Jenkins, A. & Mathiot, P. An assessment of basal melt parameterisations for Antarctic ice shelves. *Cryosphere* **16**, 4931–4975 (2022).
247. Muntjewerf, L. et al. Description and demonstration of the coupled Community Earth System Model v2 - Community Ice Sheet Model v2 (CESM2-CISM2). *J. Adv. Model. Earth Syst.* **13**, e2020MS002356 (2021).
248. Siahaan, A. et al. The Antarctic contribution to 21st-century sea-level rise predicted by the UK Earth System Model with an interactive ice sheet. *Cryosphere* **16**, 4053–4086 (2022).
249. Diener, T. et al. Acceleration of dynamic ice loss in Antarctica from satellite gravimetry. *Front. Earth Sci.* **9**, 741789 (2021).
250. Ivins, E. R. et al. Antarctic contribution to sea level rise observed by GRACE with improved GIA correction. *J. Geophys. Res. Solid Earth* **118**, 3126–3141 (2013).
251. Sasgen, I. et al. Antarctic ice-mass balance 2003 to 2012: regional reanalysis of GRACE satellite gravimetry measurements with improved estimate of glacial-isostatic adjustment based on GPS uplift rates. *Cryosphere* **7**, 1499–1512 (2013).
252. Peltier, W. R., Argus, D. F. & Drummond, R. Space geodesy constrains ice age terminal deglaciation: the Global ICE-6G_C (VM5a) model. *J. Geophys. Res. Solid Earth* **120**, 450–487 (2015).
253. Khan, S. A. et al. Geodetic measurements reveal similarities between post-Last Glacial Maximum and present-day mass loss from the Greenland Ice Sheet. *Sci. Adv.* **2**, e1600931 (2016).
254. McKay, R. M. et al. in *Antarctic Climate Evolution* 2nd edn, (eds Florindo, F. et al.) 41–164 (2022).
255. Dorschel, B. et al. The International Bathymetric Chart of the Southern Ocean version 2. *Sci. Data* **9**, 275 (2022).
256. Box, J. E. Greenland Ice Sheet mass balance reconstruction. Part II: surface mass balance (1840-2010). *J. Clim.* **26**, 6974–6989 (2013).
257. Eyring, V. et al. Overview of the Coupled Model Intercomparison Project Phase 6 (CMIP6) experimental design and organization. *Geosci. Model Dev.* **9**, 1937–1958 (2016).
258. Box, J. E. et al. Greenland Ice Sheet rainfall climatology, extremes and atmospheric river rapids. *Meteorol. Appl.* **30**, e2134 (2023).

259. Mouginot et al. Forty-six years of Greenland Ice Sheet mass balance from 1972 to 2018. *Proc. Natl Acad. Sci. USA* **116**, 9239–9244 (2019).
260. Sasgen et al. Arctic glaciers record wavier circumpolar winds. *Nat. Clim. Chang.* **12**, 249–255 (2022).
261. Hersbach, H. et al. The ERA5 global reanalysis. *Q. J. R. Meteorol. Soc.* **146**, 1999–2049 (2020).
262. Kanamitsu, M. et al. NCEP-DOE AMIP-II reanalysis (R-2). *Bull. Am. Meteorol. Soc.* **83**, 1631–1643 (2002).
263. Kobayashi, S. et al. The JRA-55 reanalysis: general specifications and basic characteristics. *J. Meteorol. Soc. Jpn* **93**, 5–48 (2015).
264. Gelaro, R. et al. The Modern-Era Retrospective analysis for Research and Applications, version 2 (MERRA-2). *J. Clim.* **30**, 5419–5454 (2017).

Acknowledgements

The authors are grateful to the World Climate Research Programme's Climate & Cryosphere core project, the International Arctic Science Committee and SCAR for co-sponsoring an ISMASS workshop that led to this collaboration. E.H. and A. Silvano acknowledge funding from NERC (NE/W005875/1, NE/Y000129/1 and NE/V014285/1). F.D.W.C. acknowledges funding from the Prince Albert II of Monaco Foundation. R.R. was supported by the TiPACCs project, which receives funding from the European Union's Horizon 2020 research and innovation programme under grant agreement number 820575. J.D.R. was supported by a UKRI Future Leaders Fellowship (grant agreement no MR/W011816/1). H.G. received funding from the EU's Horizon 2020 Research and Innovation Programme under grant agreement number 869304, PROTECT and the Research Council of Norway under projects 295046 and 324639. L.D.S. acknowledges funding from the PNRA19_00022 project. F.C. acknowledges funding from the PNRA18_00002 project and from the SCAR INSTANT Programme. R.M. received funding from the EU's Horizon Europe Programme under grant agreement number 101060452, OCEAN:ICE. I.S. acknowledges funding by the Helmholtz Climate Initiative REKLIM (Regional Climate Change), a joint research project of the Helmholtz Association of German Research Centres (HGF). A.G. acknowledges financial support from the New Zealand Ministry for Business Innovation and Employment (grant number ANTA1801; Antarctic Science Platform). The authors thank S. Hanna for the help with figure preparation.

Author contributions

E.H. designed and co-ordinated the Review and raised support for the ISMASS workshop. E.H., J.E.B., S.B., F.D.W.C., C.H., M.M., D.T., L.D.S. and A. Silvano led the writing, and all authors contributed to the writing and discussion of ideas. I.S. designed Fig. 1, D.T. designed Figs. 2 and 5, F.C. designed Fig. 3 and J.E.B. designed Fig. 4.

Competing interests

The authors declare no competing interests.

Additional information

Peer review information *Nature Reviews Earth & Environment* thanks Tom Cowton, Deborah Verfaillie and the other, anonymous, reviewer(s) for their contribution to the peer review of this work.

Related links

Argo: https://argo.ucsd.edu/
ESA Harmony: https://www.eoportal.org/satellite-missions/harmony
MEOP: https://www.meop.net/
NISAR: https://nisar.jpl.nasa.gov/
RINGS: https://www.scar.org/science/rings/about/

[1]Department of Geography, University of Lincoln, Lincoln, UK. [2]Institute for Geological and Geochemical Research, HUN-REN Research Centre for Astronomy and Earth Sciences (MTA-Centre of Excellence), Budapest, Hungary. [3]Earth and Life Institute, Université catholique de Louvain, Louvain-la-Neuve, Belgium. [4]Geological Survey of Denmark & Greenland, Copenhagen, Denmark. [5]School of Earth & Environmental Sciences, University of Cardiff, Cardiff, UK. [6]Department of Geography and Environmental Sciences, Northumbria University, Newcastle Upon Tyne, UK. [7]Airbus Defence and Space Ltd, Newcastle Upon Tyne, UK. [8]Niels Bohr Institute, University of Copenhagen, Copenhagen, Denmark. [9]Department of Earth Sciences, Dartmouth College, Hanover, NH, USA. [10]Section of Geophysics, National Institute of Oceanography and Applied Geophysics, Trieste, Italy. [11]Ocean and Earth Science, National Oceanography Centre, University of Southampton, Southampton, UK. [12]Department of Geosciences, Alfred Wegener Institute Helmholtz Centre for Polar and Marine Research, Bremerhaven, Germany. [13]Institute of Geography, University of Augsburg, Augsburg, Germany. [14]Cooperative Institute for Research in Environmental Sciences (CIRES), University of Colorado Boulder, Boulder, CO, USA. [15]Institute for Marine and Atmospheric Research Utrecht, Utrecht University, Utrecht, The Netherlands. [16]Department of Earth, Geographic, and Climate Sciences, College of Natural Sciences, University of Massachusetts Amherst, Amherst, MA, USA. [17]Norce Norwegian Research Centre, Bjerknes Centre for Climate Research, Bergen, Norway. [18]Antarctic Research Centre, Te Puna Pātiotio, Victoria University of Wellington, Te Herenga Waka, Wellington, Te Whanganui-a-Tara, Aotearoa New Zealand. [19]Division of Research and Educational Support, Mid Sweden University, Östersund, Sweden. [20]Norwegian Polar Institute, Tromsø, Norway. [21]School of Geosciences, University of Edinburgh, Edinburgh, UK. [22]National Centre for Climate Research, Danish Meteorological Institute, Copenhagen, Denmark. [23]Departement of Geosciences, Environnement, Society, Université Libre de Bruxelles, Brussels, Belgium. [24]Department of Earth System Science, University of California Irvine, Irvine, CA, USA. [25]Department of Civil and Environmental Engineering, University of California Irvine, Irvine, CA, USA. [26]Radar Science and Engineering Section, Jet Propulsion Laboratory, Oak Drive, CA, USA. [27]Department of Earth Science, Barkatullah University, Bhopal, India. [28]Department of Geological Sciences and Engineering, University of Nevada, Reno, NV, USA. [29]Department of Geography, University of Sheffield, Sheffield, UK. [30]Department of Earth and Climate Sciences, Middlebury College, Middlebury, VT, USA.